tyco corporate technology center

Contract No. NAS8-29031

CARBON MONOXIDE DETECTOR

Final Report

Covering Period: 26 June 1972 - 25 June 1973

December 1973

(NASA-CR-120171) CARBON MONOXIDE DETECTOR Final Report, 26 Jun. 1972 - 25 Jun. 1973 (Tyco Labs., Inc.) 68 p HC $6.50 CSCL 14B

N74-20012

G3/14 Unclas 16497

Prepared for

George C. Marshall Space Flight Center
National Aeronautics and Space Administration
Marshall Space Flight Center, Alabama 35812

A Division of Tyco Laboratories, Inc
16 Hickory Drive, Waltham, Massachusetts 02154

Contract No. NAS8-29031

CARBON MONOXIDE DETECTOR

Final Report

Covering Period: 26 June 1972 - 25 June 1973

Tyco Laboratories, Inc.
16 Hickory Drive
Waltham, Massachusetts 02154

by

G. L. Holleck
J. L Bradspies
S. B. Brummer
L. L. Nelsen

December 1973

Prepared for

George C. Marshall Space Flight Center
National Aeronatics and Space Administration
Marshall Space Flight Center, Alabama 35812

ABSTRACT

An electrochemical sensor has been developed to continuously and accurately monitor ppm levels of carbon monoxide in air. The device is based on the electrochemical oxidation of carbon monoxide in a "fuel cell" type detector. For high sensitivity and stable operation, various parameters such as operating potential, electrode structure, electrolyte, gas humidity, cell construction, etc. have to be suitably selected and controlled.

The presence of air limits the potential of operation to between approximately 1.0 and 1.4 V versus RHE. In phosphoric acid, one of the electrolytes investigated, the CO oxidation current on Teflon-bonded platinum electrodes is practically independent of potential within this range. However, the current is not diffusion controlled and it decays with time. At least two mechanisms are responsible for this decline in signal: (1) a slow increase and/or rearrangement of the oxide on the electrode surface, and (2) a slow accumulation of an intermediate of a side reaction which acts as an electrode "poison." The temperature dependence of the CO oxidation follows an Arrhenius equation with an activation energy of 6.5 kcal/mole.

The oxidation of CO in a sulfuric acid electrolyte shows significant differences: The current is higher than with H_3PO_4 and is potential dependent. The rate of current decrease during continuous CO sampling also is a function of operating potential. A stable detection current is obtained in the lower potential region (~1 V versus RHE), while at higher potentials the signal declines. The activation energy of the CO oxidation in sulfuric acid was determined as 4 kcal/mole at 1.2 V and 2.6 kcal/mole at 1.0 V versus RHE.

The CO oxidation current was found to be fairly insensitive to variation in electrolyte concentration. However, the electrolyte level and thus the humidity of the gas sample have to be suitably controlled to prevent drying

or flooding of the electrode. A special cell design has been developed that can tolerate appreciable humidity variations without effect on the CO detection current. This eliminates the need for special humidity controls in a space capsule environment, where the humidity can vary between 8 and 12 torr H_2O vapor and reduces the humidity control requirements for terrestrial use.

Based on the above data, a complete CO monitoring system has been constructed and tested. The potential is controlled by a potentiostatic circuit using a palladium reference electrode.

Table of Contents

Table of Contents (continued)

List of Illustrations

List of Illustrations (continued)

List of Illustrations (continued)

I. INTRODUCTION

The detection of noxious or inflammable gases such as CO is a serious problem in industrial environments, in mines, and for spacecraft applications. In many cases what is required is a rugged, sensitive, and preferably inexpensive detector-alarm system which will respond to the presence of small amounts of the undesired contaminant. Then, with an appropriate sampling manifold, the device may be used to monitor continuously for the presence of a noxious gas and, if desired, a portable instrument may be used to "sniff out" the source of the gas.

The physiologically active CO concentrations are in the ppm range. Generally, a CO concentration of 100 ppm is regarded as an upper tolerable limit for long-term exposure.

The aim of this contract was to develop a sensitive CO detector specifically for spacecraft use. Under normal operation, no significant CO concentrations should be present in the space capsule; therefore, an instrument range of 0 to 60 ppm CO in air was devised. Further, the CO detector should be able to accurately and continuously monitor the CO concentration throughout the whole mission, that is, for several weeks, without requiring recalibration. A sudden increase in the CO level could then indicate a malfunction in the spacecraft, e.g., charing of insulation, etc. The normal environmental conditions in the space capsule would include a temperature between 65 and 75°F and dew points between 46 and 57°F. Even though no direct flight hardware was to be built, special consideration had to be given to the space environment that is operation independent of orientation and in zero gravity.

A fuel cell type detector used as a high sensitivity electrolysis cell appeared to be particularly well suited for this application, and the development of a practical electrochemical CO monitor was the purpose of this program.

In the following we discuss the concept of an electrochemical CO detector and we report on the CO oxidation behavior in phosphoric and sulfuric acid electrolyte. Based on the conclusion of the experimental results, we have built a complete portable bench prototype CO detector which was delivered to the George C. Marshall Space Flight Center.

II. CONCEPT OF AN ELECTROCHEMICAL GAS DETECTOR

The principle of the electrochemical detection of materials involves their reactions at an electrode. For example, gaseous CO can be oxidized to CO_2 according to:

$$CO + H_2O \xrightarrow{\text{Pt electrode}} CO_2 + 2\,H^+ + 2\,e^-, \qquad (1)$$

and two electrons can be detected in the external circuit for each CO molecule which is oxidized.

This method of detection is extremely sensitive because one equivalent of material releases one Faraday (96, 500 coulombs) when electrolyzed. Since it is a simple matter to detect a microcoulomb of charge, it is easy to detect 10^{-11} equivalents of a material. It is not usually convenient, however, to measure the charge passed in electrolyzing a contaminant, and rather, one prefers to measure the current passing during the electrolysis.

Some of the difficulties in attempting to do this, e.g., for active fuels like H_2 or CO, may be illustrated by reference to Fig. 1. This figure represents the observed current-potential relationships for the oxidation of H_2 [reaction (2)] and also shows (in Fig. 1b) the reduction of O_2 [reaction (3)] in acid solutions at Pt electrodes.

$$H_2 \xrightarrow{\text{Pt electrode}} 2\,H^+ + 2\,e^- \qquad (2)$$

$$O_2 + 4\,H^+ + 4\,e^- \xrightarrow{\text{Pt electrode}} 2\,H_2O \qquad (3)$$

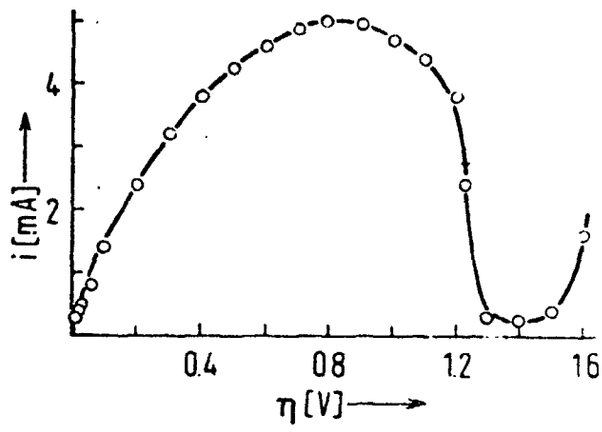

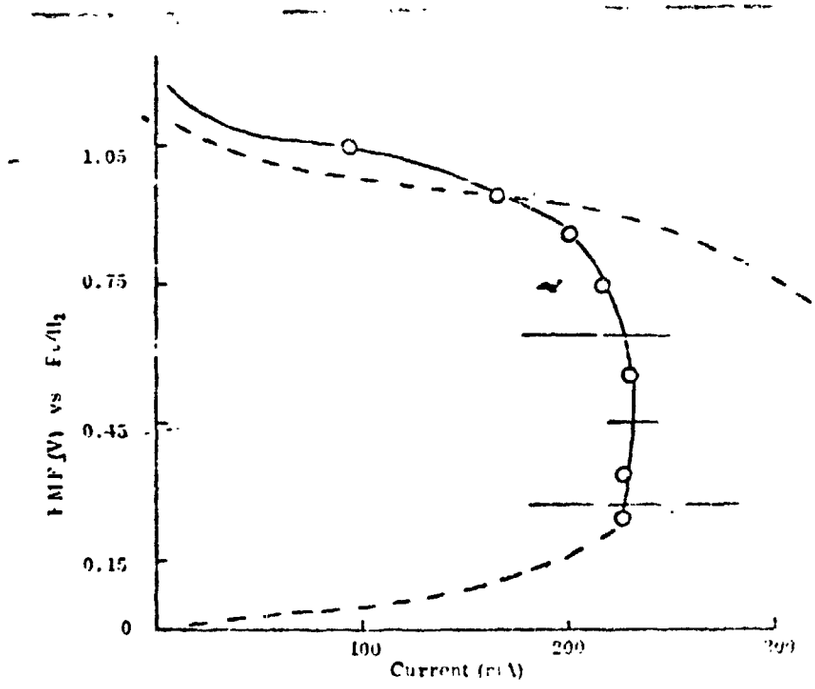

Fig. 1. (a) Current-potential curve for H_2-oxidation on partially immersed platinum electrodes in acid solution.[1] (b) Current-potential curve for H_2-oxidation on platinum fuel cell electrode. Dotted line starting at 1.1 V represents O_2-reduction[2]

Active fuels like H_2 or CO oxidize very closely to their reversible potentials and, as the driving force for the reactions is increased, i.e., at higher potentials, the rate of oxidation increases sharply. Finally, the oxidation rate becomes limited by the rate at which the fuel diffuses to the surface of the electrode (e.g., on the fuel cell electrode from ~0.2 to ~0.6 V). Then the oxidation rate is directly proportional to the fuel pressure and is independent of the potential. These are the ideal conditions for operating an analytical device.

The reduction of O_2 is much less reversible than fuel oxidation so that it does not start at 1.23 V versus the H_2 electrode, which is the reversible potential for reaction (3). Significant reduction starts to occur at about 1.1 V and accelerates as the potential is lowered. Finally, at low potentials, O_2 reduction is limited by diffusion (not shown). It is clear, then, that any effort to detect small amounts of fuel in the presence of air would be rather difficult because of the tendency for O_2 reduction from the air to mask the fuel oxidation current. To avoid this problem, the potential of the sensing electrode must be set above the region where the O_2 reaction occurs.

The crucial decisions in the practical use of such a device relate to the choice of electrode structure and arrangement, to electrolyte reference electrode and control systems, as well as to the arrangement of the electrolyte water balance. These factors influence directly the sensitivity, accuracy, and stability of a practical CO detector and thus were the main subjects of this investigation.

III. EXPERIMENTAL DATA

A. Test Setup and Procedure

A schematic flow chart of the test procedure is shown in Fig. 2. Individual steps and procedures were modified and improved during the course of the program, so, e.g., several electrochemical cell designs were used and are described in more detail later. The test gas consisted of commercially available CO-air mixtures (Airco). The gas was used either directly from the cylinder or diluted to the desired concentration with air in a gas mixer. The gas mixing arrangement consisted of a system of calibrated glass capillaries and oil manometers which allowed one to accurat measure the pressure drop across the capillaries upon gas flow. Thus, the relative flow velocities of the two gas streams (CO-air and air) could be accurately determined and maintained. It was found most practical to use a stock gas mixture containing 200 or 500 ppm CO in air and to dilute it with air to the test gas concentration of 10 to 100 ppm CO. The test gas then passed through two prehumidifiers to equilibrate it with the same partial pressure of water that corresponds to that of the electrolyte at the temperature of the electrochemical detector cell. The prehumidifiers consisted of 2 two-liter double mantle flasks. The first flask contained triply distilled water and was thermostatted by means of a Haake recirculator to a temperature at which the water vapor pressure was equal to that of the electrolyte in the test cell. The second flask contained the same electrolyte at the same temperature as employed in the test cell. The gas stream entered the presaturators through a submerged glass frit. Standard flow meters (Dwyer) were used to determine the gas flow rate. It was, in general, between 0.5 and 2 SCF/hr.

During the course of our investigation, we used two different cell desig which are described in more detail in the following sections. The electrochem cells were thermostatted between 10 and 35°C in a controlled atmosphere chamber.

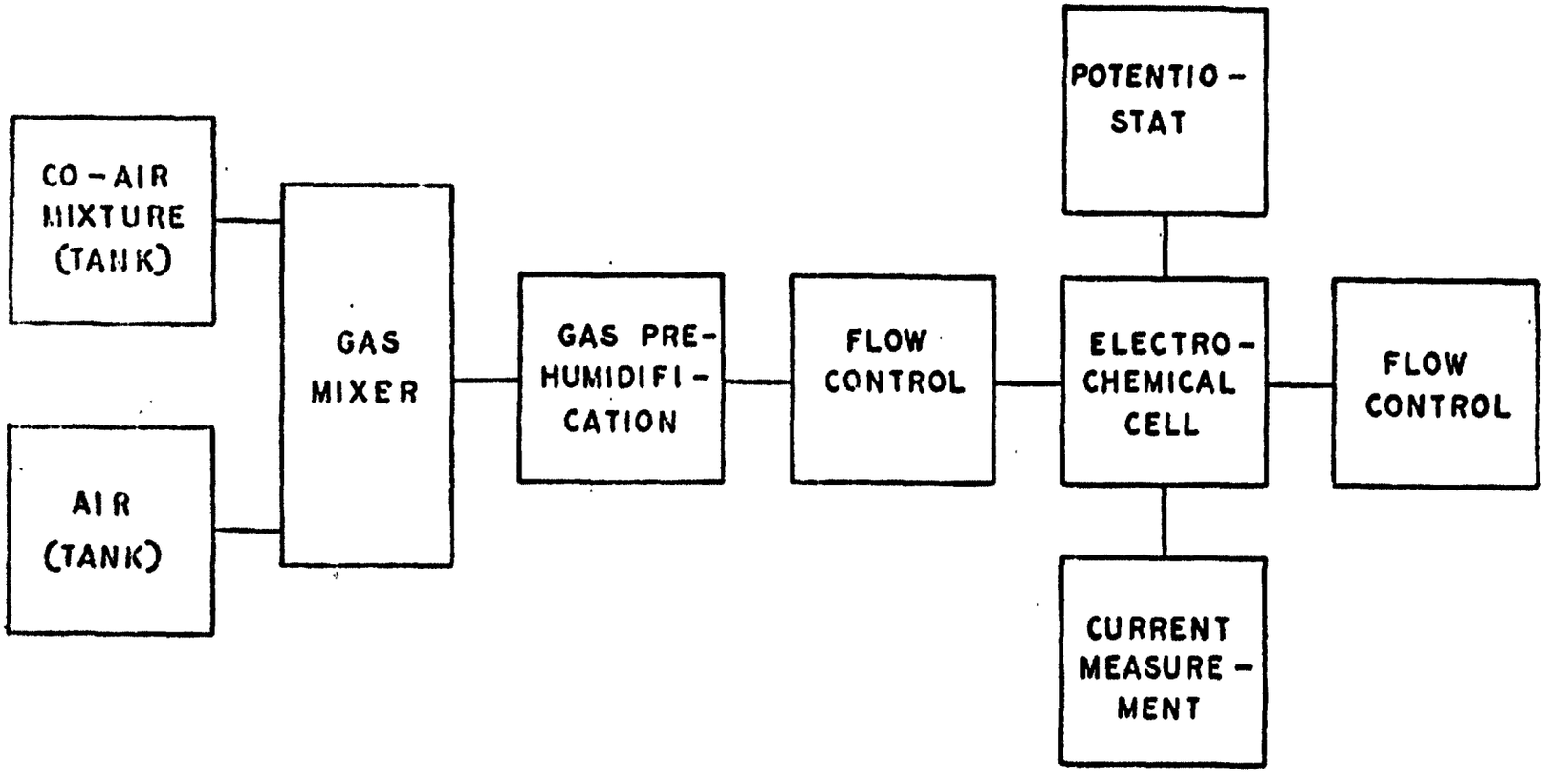

Fig. 2. Schematic flow chart of test procedure

The electrode potential was controlled by a potentiostat (Wenking) and the detection current was continuously recorded (strip chart recorders, Sargent and Moseley models MR and 7100B, respectively).

For long-term stability measurements, the gas stream passed through two electrochemical cells in series. Each cell had its own electronic control and measuring circuits. Thus, it was possible to determine whether small changes in the cooxidation current resulted from variations in the test gas or from changes in the detector cell and/or its electronic control and measuring circuit.

Phosphoric acid (Fisher, reagent) and sulfuric acid (Baker, reagent) were used as electrolytes. The electrolyte concentration was chosen such that its water vapor pressure at the operating temperature was approximately that of the space capsule environment. Thus, concentrations of 55 to 63% were used for phosphoric and approximately 40% for sulfuric acid.

The working and counter electrode consisted of Teflon-bonded platinum black on gold plated tantalum screen. They were prepared with various platinum loadings and Teflon content at Tyco. In addition, we used some electrodes from Unican Limited and ERC, Inc. In general, the electrodes were subjected to anodic and cathodic cycles in sulfuric acid in order to remove traces of impurities or wetting agents. This was followed by repeated washing in hot distilled water.

Modifications of this general test procedure and specific experimental techniques are described in conjunction with the experimental results.

B. Initial Cell Design

For our initial measurements, we used an electrochemical detector assembly, as shown in Fig. 3. This cell was used with two rather than the standard three electrodes applied in potentiostatted systems: the working

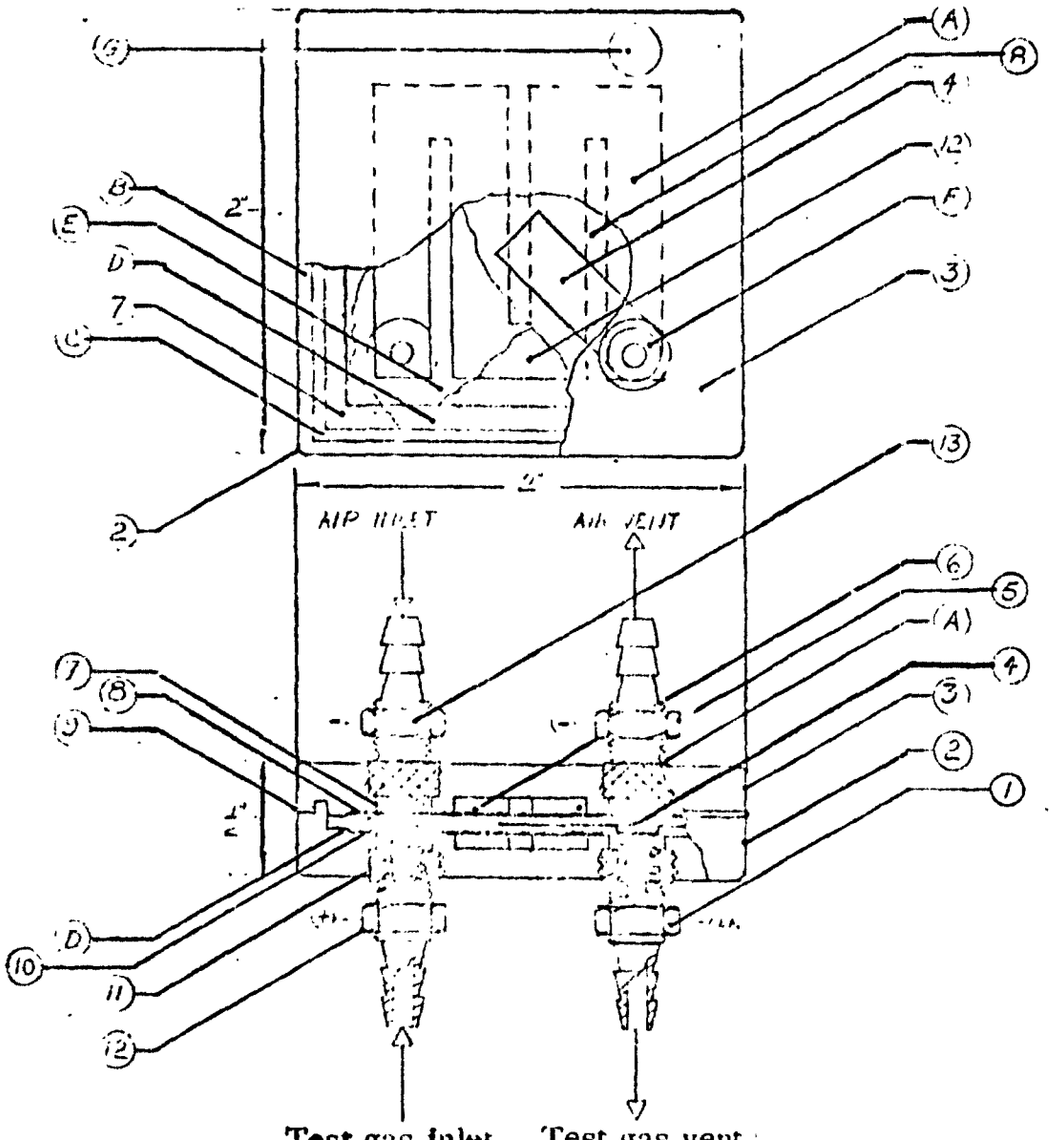

COMPONENT PARTS

Part No.	Description	Material
1	Reference Terminal and Gas Vent Fitting	Type 316 S.S.
2	Anode End Plate	Glass Filled Teflon
3	Cathode End Plate	Glass Filled Teflon
4	Reference Electrode	-
5	Mounting Stud and Air Vent Fitting	Type 316 S.S.
6	Cathode-Oxygen Counter Electrode	Platinum Black Mesh
7	Separator (notched for reference contact clearance) electrolyte saturated	Glass Felt - Phosphoric Acid
8	Separator-electrolyte saturated	Glass Felt - Phosphoric Acid
9	Adhesive Seal	Epoxy
10	Anode-CO sensing electrode (notched for reference contact clearance)	Platinum Black Mesh
11	Contact Spring	Type 316 S.S.
12	Positive terminal and gas inlet fitting	Type 316 S.S.
13	Negative terminal and air inlet fitting	Type 316 S.S.

FEATURES

Features	Description
A	Flow Channel
B	Adhesive Seal Land
C	Separator Compression Control Ridge
D	Separator Compression Land
E	Electrode Support Land
F	Terminal (fitting) Cast Insert Assembly
G	Antirotation Mounting Boss

Scale: 2 x
By: S. Mermelstein
Date: 5/12/71

Fig. 3. Electrochemical detector assembly

electrode at which CO is oxidized, and the counter electrode which also functions as the reference electrode. The working and counter/reference electrode were identical platinum black-Teflon-"fuel cell electrodes" on a gold plated tantalum current collector screen. The electrodes were separated in the cell by a fiber glass matrix (Gelman) which was saturated with the electrolyte. Since this cell had two separate gas manifolds for the anode and cathode, it was possible to use hydrogen gas instead of air for the counter electrode and thus obtain a well-defined reference potential while using only a two-electrode cell. The prototype detector will, however, not be operated with hydrogen, and it was therefore necessary to establish a suitable reference electrode system. This and the resulting three electrode cell designs are discussed in the following.

C. The Reference Electrode System

In order to hold the CO indicating electrode at a constant potential, it was necessary to find a suitable reference electrode. As we will see later, the absolute potential value of the working electrode is not extremely critical; however, potential changes or transients have to be kept at a minimum since they would cause considerable double layer charging currents at the high surface area Teflon-bonded, Pt-black electrodes. It would be most convenient to use the counter electrode or a separate air breathing electrode as potential reference. This possibility was examined by testing Teflon-bonded electrode structures in half-cell experiments.

The experiments were performed in a three-compartment cell which allows the working electrode to float and has a Luggin capillary from the reference compartment situated directly beneath the working electrode. The electrolyte was 55% H_3PO_4. An H_2 electrode in a separate compartment was used to maintain a reference potential. With air bubbling through the electrolyte, the cathodic current-potential curve was determined (Fig. 4) using

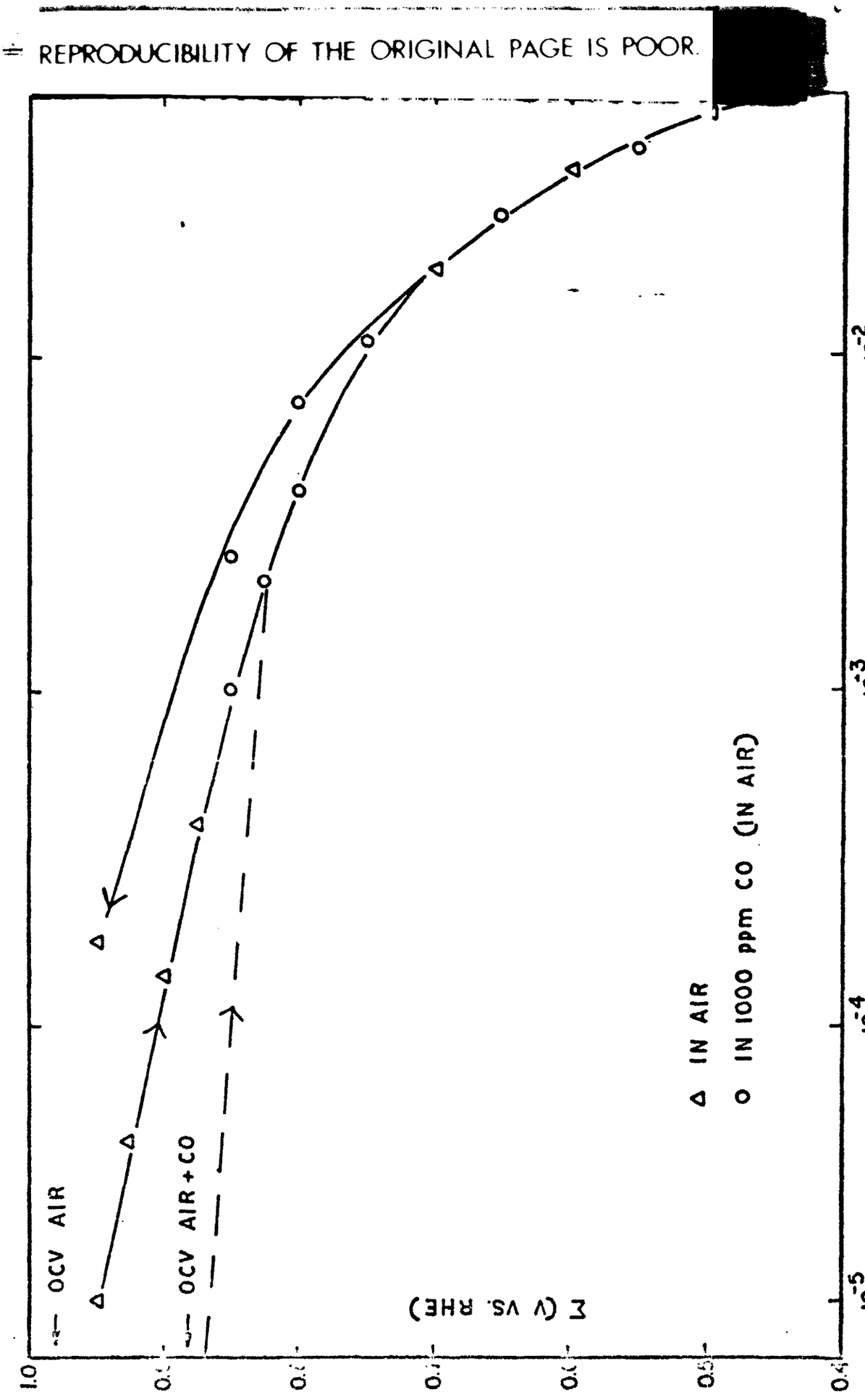

Fig. 4. Cathodic current-potential curve for Teflon-bonded Pt black electrode

a Wenking potentiostat to maintain the Teflon-bonded electrode at preset potentials. The open circuit potential of the system was +0.98 V, and the cathodic Tafel slope of the cathodic reaction (oxygen reduction) was 60 mV. Upon anodic disturbance, the electrode potential did not return to the original open circuit value, demonstrating the absence of a suitable anodic process. The experiment was then repeated using air containing 1000 ppm CO. Fig. 4 shows that in the O_2 reduction region (below 0.75 V versus RHE), the current is not noticeably affected by the presence of CO. However, the open circuit potential dropped nearly 100 mV when CO was introduced into the cell, from ~0.98 V to ~0.88 V (versus RHE). This suggests an anodic current of approximately 500 μA for CO oxidation. The lack of a suitable reaction stabilizing the potential against anodic disturbance, and the sensitivity of the open circuit potential towards the presence of carbon monoxide preclude the use of an air-breathing, Teflon-bonded platinum electrode as a potential reference.

The second electrode to be studied was bright palladium foil and palladized palladium. These studies were carried out in a standard three-compartment electrochemical cell and also used 55% H_3PO_4 as electrolyte. The open circuit potential for bright Pd was very erratic and varied in range from +0.65 to +0.75 V versus RHE. Only very small cathodic currents, i.e., of the order of 0.2 $\mu A/cm^2$, were needed to displace the potential of this electrode by as much as 100 mV. The current-potential relation for palladized Pd (shown in Fig. 5) was much more stable. The open circuit value was +0.788 V ± 2 mV, and larger currents were needed to affect an appreciable potential shift. The cathodic Tafel slope for O_2 reduction is 30 mV, as observed for the fuel cell electrode. As a further test, the electrode's sensitivity to CO was determined. There was virtually no change in the open circuit

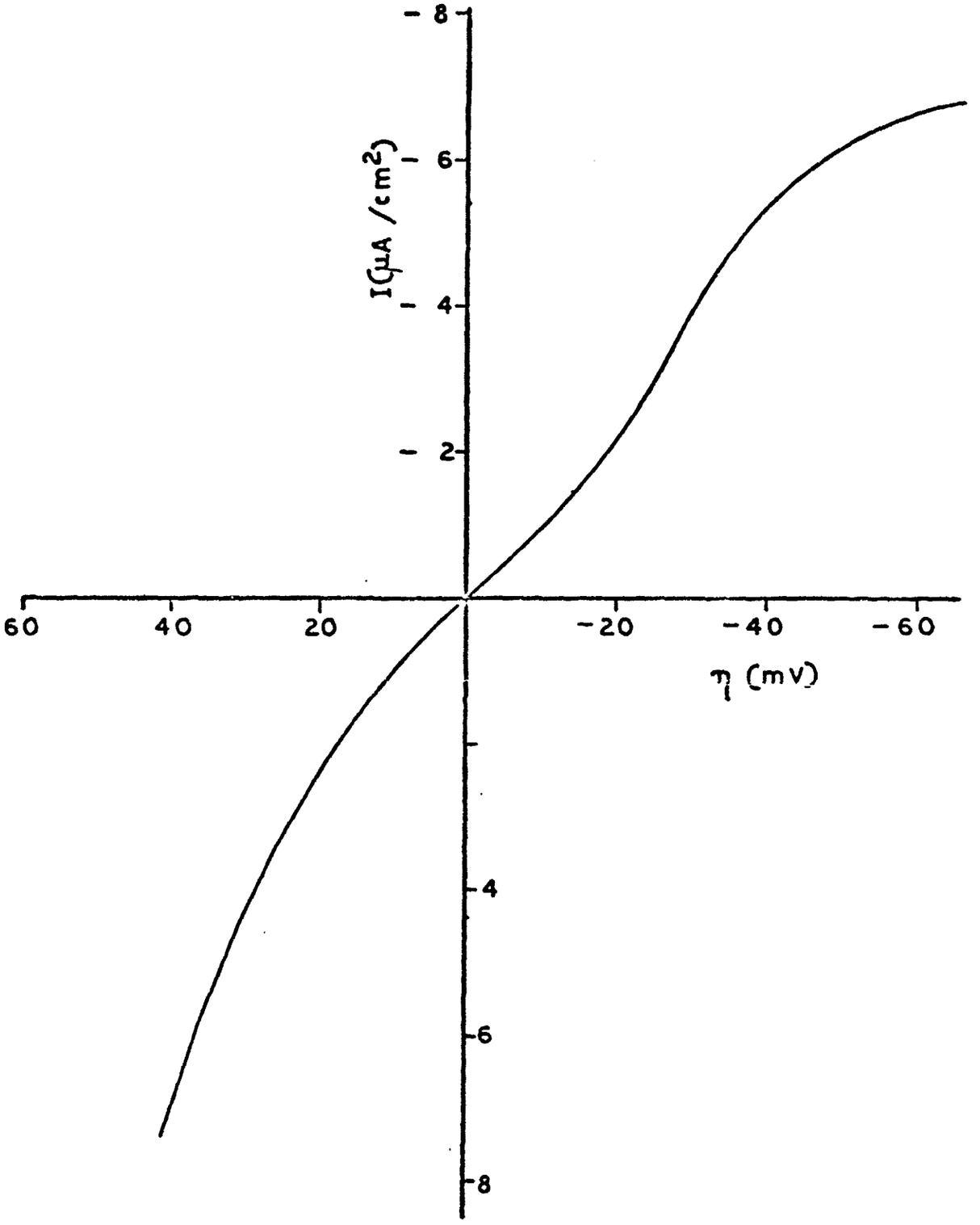

Fig. 5. Current-potential relationship of palladized Pd in 55% H_3PO_4 saturated with air or air + 100 ppm CO

value in the presence of 100 ppm CO in air. Overall, the data is practically identical to that obtained in the absence of CO.

These measurements show that a palladium electrode, especially when palladized, maintains a given open circuit potential that is fairly insensitive against small cathodic or anodic disturbances. The cathodic reaction is oxygen reduction while the anodic reaction appears to be slow palladium dissolution. Further CO, in the concentration range of interest here has no effect on the electrode potential. The same behavior was also established for a sulfuric acid electrolyte.

Based on these findings, we can conclude that a foil or wire of palladized Pd inserted in the cell matrix, to be used as a separate reference electrode, offers sufficiently accurate and stable potential control for our system.

D. Improved Cell Design

An improved CO detector cell was designed with special consideration for the planned application in a spacecraft environment. Such considerations included, simplicity, ruggedness, independence of position, and gravity as well as maximum response and signal stability. A schematic of the CO sensor cell is shown in Fig. 6.

The cell body consisted of two identical parts with circular geometry and assembled with six bolts. The material of construction was polyethylene. The Teflon-bonded Pt electrodes were held between expanded tantalum current collectors and the glass fiber electrolyte matrix. The palladium reference electrode was imbedded into the electrolyte matrix. The CO-containing air enters the cell through the center hole, passes over the CO sensing electrode, bypasses the electrochemical subcell through four gas channels, and exits at the opposite side.

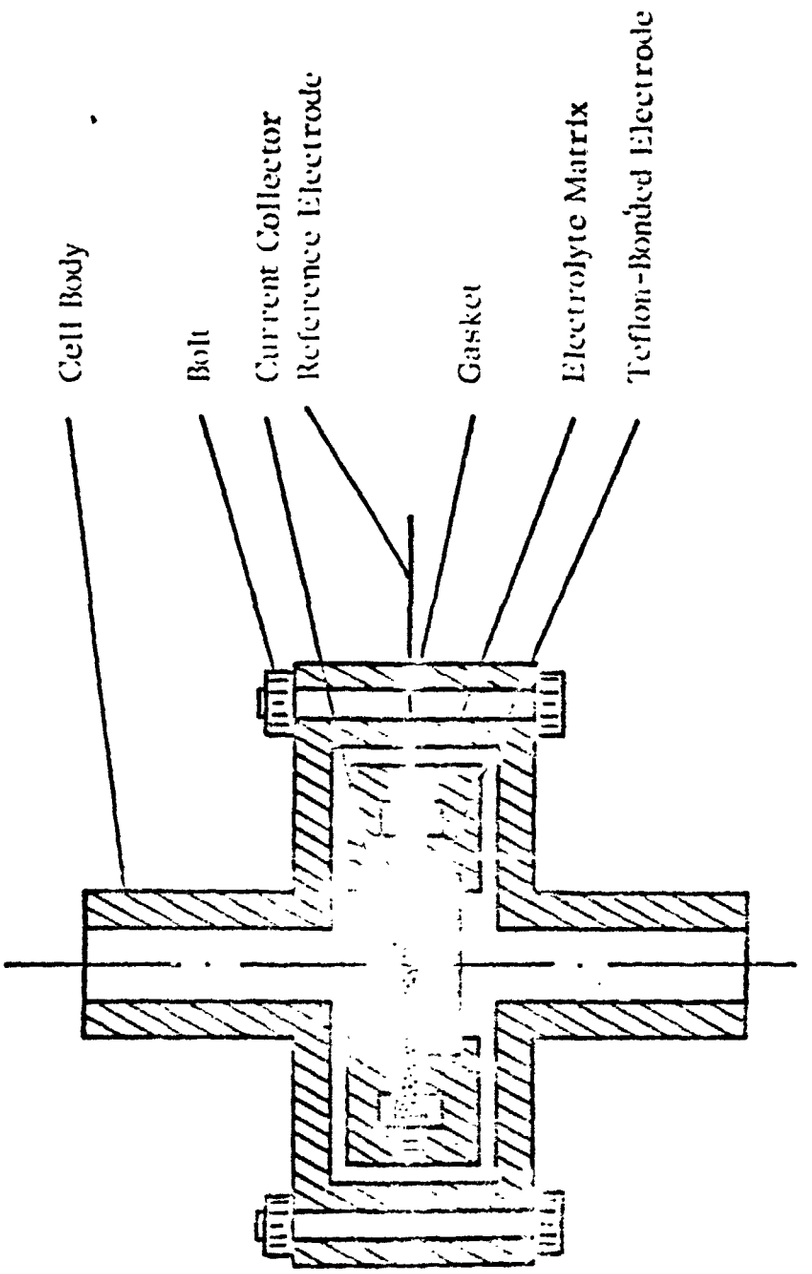

Fig. 6. Schematic of CO sensor cell

This cell has an additional design feature which is worth special mentioning. The separator extends beyond the electrodes into an open ring-shaped space. There the separator is without compression. This results in a double porosity of the electrolyte matrix with a larger average pore-size in the uncompressed outer ring. This special feature allows the operation of the cell over a large range of electrolyte volume and thus makes it fairly insensitive to humidity fluctuations in the incoming gas stream.

IV. CARBON MONOXIDE OXIDATION

A. General Considerations

We have discussed the concept of our electrochemical detector in a previous section and we have seen that for the successful development of a practical CO detector, a number of questions have to be answered. First of all, we have to select an electrode material which is catalytically active for the oxidation of CO. Platinum is one of the best electrocatalysts, and in all of our work we used platinum-based detection electrodes. Further, the catalyst has to be provided in a suitable electrode structure. To obtain sufficient sensitivity, it is necessary to provide a structure which results in a large gas-electrolyte-catalyst interface (e.g., electrodes of the Teflon-bonded, Pt-black type.) Another factor of importance is the choice of a suitable electrolyte. Generally, acid electrolytes are to be preferred since they reject the formed CO_2 as gas. We have therefore investigated phosphoric acid, which is commonly employed in acid fuel cells, and sulfuric acid as electrolytes for use in an electrochemical CO sensor.

For a given electrode and electrolyte system, we have now to define the operating conditions and determine their effect. They include potential of generation, gas flow rate, operating time, CO concentration, and operating temperature.

In the following sections we will discuss the results of our investigation regarding the effect of these parameters and their implication on a practical CO detection device, first in phosphoric acid and then in sulfuric acid.

B. Results in Phosphoric Acid Electrolyte

1. Effect of potential and gas flow rate

In initial measurements, the effect of potential and gas flow rate on the carbon monoxide oxidation current was determined. As Fig. 7 shows,

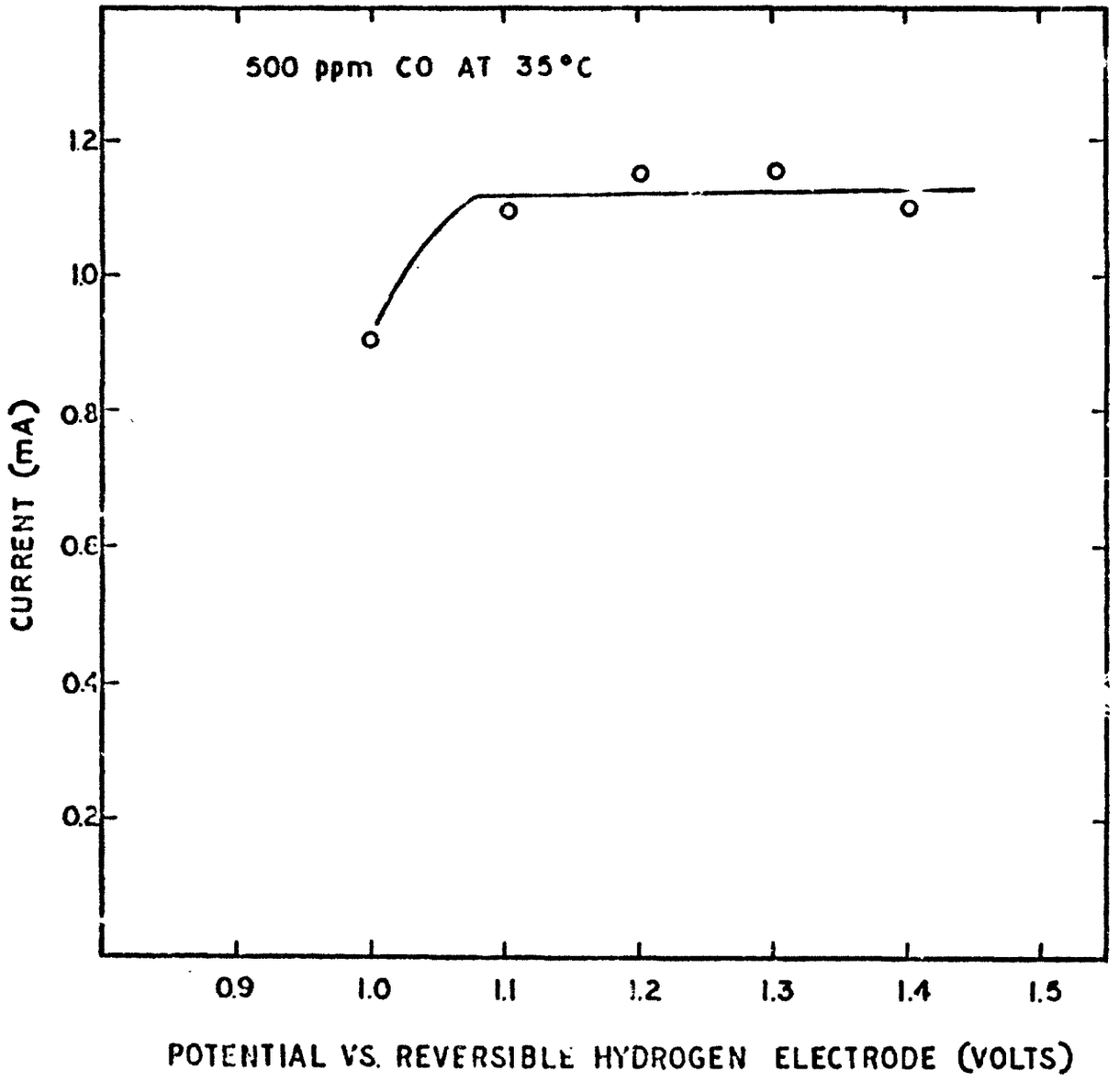

Fig. 7. Dependence of carbon monoxide oxidation current on potential

at least between 1.1 and 1.4 V versus RHE, there is very little effect of potential on the detection current. This demonstrates that electron transfer, the rate of which is strongly potential dependent, is not a limiting factor. Therefore, most of the following experiments were carried out with the working electrode potentiostatted to 1.2 V versus RHE. Since this is close to the theoretical open circuit potential of the air electrode, a minimum background current can be expected.

The flow rate of the carrier gas can affect the observed CO oxidation current. At low gas flow rates, the detector signal increased with increasing flow rate. However, above a flow rate of the carrier gas between 1 and 2 SCF/hr, the CO oxidation current became independent of the flow rate. Therefore, most further measurements were carried out at 2 SCF/hr.

2. Effect of time

A typical example of an early current time curve obtained at a fresh platinum electrode is shown in Fig. 8. During the first hours of continuous CO sampling, the current declined fairly rapidly. This was then followed by a further slow decrease in detection current. As will be shown later, humidity changes in the feed gas cannot account for this signal decline.

Further experiments showed that the initial current decay on fresh electrodes (pre-equilibrated in humidified air at 1.2 V versus RHE for 2 to 3 hr after which the background current was less than 10 μA) was dependent on the CO concentration. A current time-curve for 200 ppm CO in air is shown in Fig. 9. The effect of CO concentration on the amount and rate of current decline is further summarized in Table I.

Additional observations which were made on this current decline are as follows:

1. The current cannot be restored to its initial high values by flushing with carbon monoxide-free air for periods up to 12 hr.

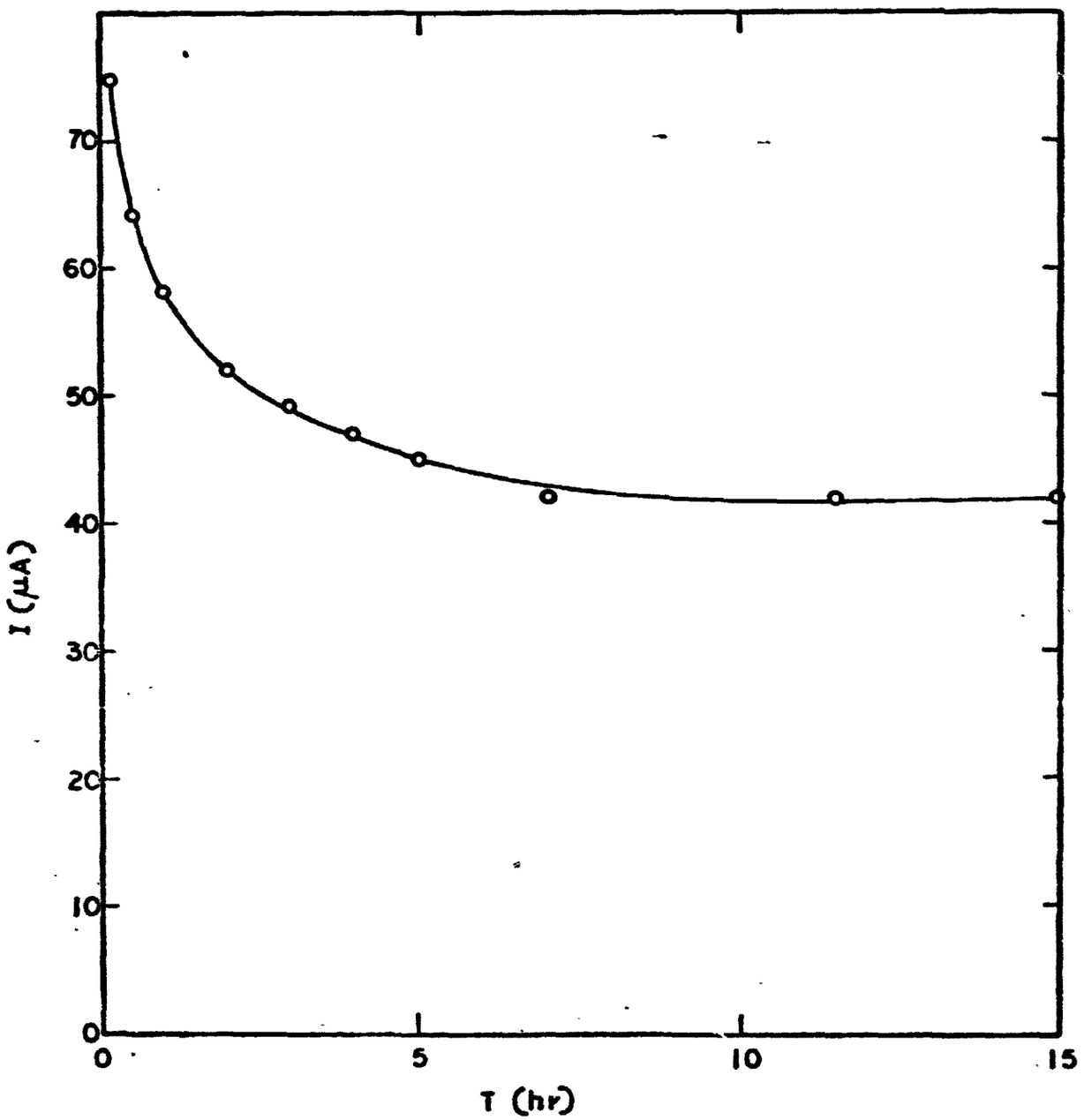

Fig. 8. Detection current for 50 ppm CO on an initially CO-free electrode

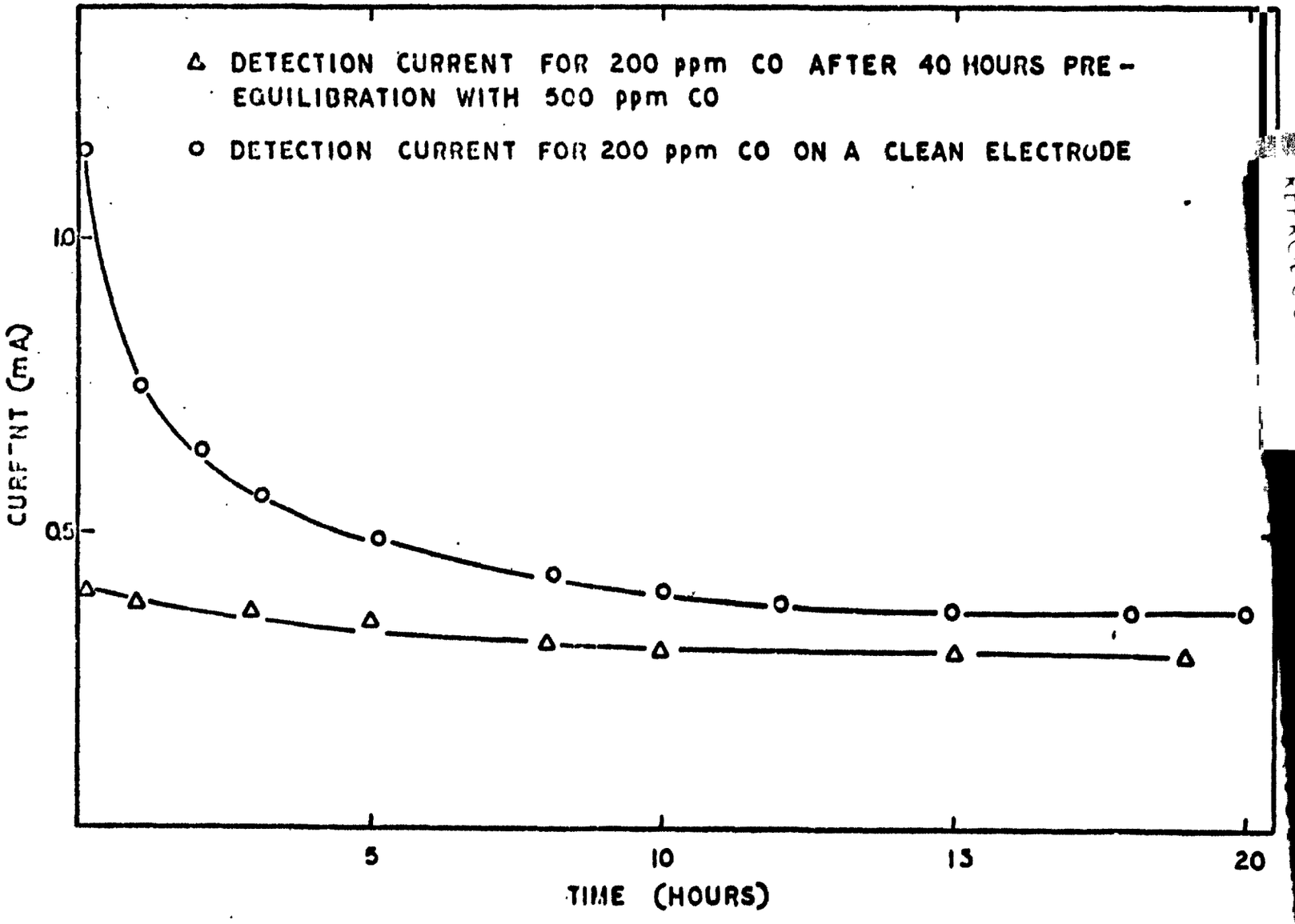

Fig. 9. Effect of pre-equilibrating the electrode with higher concentrations of carbon monoxide

Table I. Effect of Carbon Monoxide Concentration on Amount and Rate of Current Decline

CO Concentration	Final Current / Initial Current	Steady-State Current
50 ppm	0.57	7 hr
200 ppm	0.36	12 hr
500 ppm	< 0.18	> 30 hr

2. Once the detection current has reached a steady-state value (e.g., after 6 to 10 hr for 50 ppm CO), shutting off the CO stream and then re-introducing it results in a new detection current nearly equal to the previous steady-state value, with little further decline.

3. Prior exposure of the electrode to CO concentrations higher than the measured concentration results in initial currents much lower than initial currents observed on "clean" electrode surfaces, but does not significantly change the final steady-state detection current. (See Fig. 9 where the detection current for 200 ppm CO is shown on a "clean" electrode and on an electrode which had been equilibrated at 1.2 V with 500 ppm CO.) Mor importantly, if the electrode is equilibrated for long periods of time with high concentrations and then used to detect low concentrations, the "steady-state" detection current for the low CO concentration is reached with very short times and little further current decline is observed.

4. Prior "aging" of the electrode surface by equilibration at 1.2 V with carbon monoxide-free air for periods of 12 to 20 hr results in lower initial currents, but does not significantly change the steady-state current.

These observations are all roughly consistent with a theory of poisoning of the electrode by either carbon monoxide or a product of the oxidation of carbon monoxide. Stonehart[3] reports a poisoning of platinum and gold electrodes by a reaction product formed by a side reaction in the oxidation of carbon monoxide at 1.2 V versus RHE.

According to Stonehart, the major reaction of carbon monoxide at a platinum surface at 1.2 V is oxidation to carbon dioxide by a direct two-electron transfer reaction (this is presumably the reaction which determines the detection current):

$$CO + H_2O \xrightarrow{k_1} CO_2 \uparrow + 2H^+ + 2e^- \qquad (4)$$

However, Stonehart also postulates another parallel (but minor) reaction route from CO to CO_2 which proceeds via a one-electron reaction intermediate, CO^+:

$$CO \xrightarrow{k_3} CO^+ (\text{adsorbed}) + 1e^- \qquad (5)$$

$$CO^+ (\text{adsorbed}) + H_2O \xrightarrow{k_3} CO_2 \uparrow + 2H^+ + 1e^- \qquad (6)$$

Stonehart's data (obtained on rotating disc electrodes) support the hypotheses that the reaction intermediate, CO^+, adsorbs strongly on the electrode and that the rate-limiting step in the conversion of CO to CO_2 via this second reaction is the oxidation and desorption of the reaction intermediate, CO^+. This reaction mechanism would lead to a steady-state

concentration of CO^+ adsorbed on the electrode surface, and it is hypothesized that sites upon which CO^+ is adsorbed are not available for the primary CO oxidation route (Reaction 4). Thus, the decline in current (and its eventual leveling out) can be explained as a building up of the CO^+ "poison" on the platinum electrode until it reaches a steady-state value where the rate of desorption (Eq. 3) is equal to the rate of adsorption (Eq. 5). This steady-state coverage of the electrode by the poison can be related to the concentratio of CO in the gas stream by setting Reactions (5) and (6) equal to each other with the following assumptions:

a. The rate of Reaction (5) is proportional to the CO concentration in the gas stream and to the number of unpoisoned sites remaining on the electrode.

b. The rate of Reaction (6) is proportional to the fractional coverage of the electrode by CO^+.

Thus, at steady-state:

Adsorption = Desorption

$$k_2 (1-\Theta) [CO]_{gas} = k_3\Theta \qquad (7)$$

Steady-state fractional coverage is represented by:

$$\Theta = \frac{k_2 [CO]_{gas}}{k_3 + k_2 [CO]_{gas}} \qquad (8)$$

As can be seen, the steady-state fractional coverage by the "poisoning" species, CO^+, increases as the concentration of CO in the gas increase. This result is consistent with the greater percentage decline observed with high feec

concentrations than with lower ones. This hypothesis would also explain non-linearity of the steady-state currents with concentration, as will be shown later. According to the "poisoning" equations developed above, the number of electrode surface sites available for CO oxidation would be lower at higher CO concentrations because of greater "poisoning" by CO^+.

One conclusion emerging from these data is that high concentrations of CO (which were used for convenience in initial experiments) are not adequate models for CO detection in lower concentration ranges (e.g., 50 ppm and below) because of differences in the amount of "poisoning" at higher concentrations. The CO^+ poisoning model implies that at sufficiently low concentrations there should be little coverage of the electrode surface by CO^+ and that, therefore, the current in these low concentrations should be more linear with concentration and should show less decline with time.

There is considerable evidence that the rate of desorption of the poisoning species is extremely slow. For example, flushing of electrodes with air does not restore the initial high currents. In addition, when electrodes have first been pre-equilibrated with high concentrations of CO, the detection current on low CO concentration feeds is quite stable: it neither declines with time (i.e., is further poisoned) nor rises with time (which would indicate desorption to equilibrate with lower concentrations). These findings offer the intriguing possibility that a stable surface for detection of low concentrations (0 to 100 ppm, for example) could be produced by first equilibrating the electrodes with a CO concentration much higher than would need to be detected. If the equilibrium concentration of "poison" from this high concentration feed stream then remained stably adsorpbed, presumably no further adsorption from lower concentrations would occur, and the detection currents for lower concentration feed streams would remain stable.

This effect is shown in Fig. 10, where the electrode was first exposed to a "high" concentration of CO of 200 ppm (curve A) and then used to detect a lower concentration of 50 ppm carbon monoxide (curve B). There was no current decline observed with the 50 ppm feed.

A more rigorous investigation of this effect showed, however, that even though the desorption of the inhibiting species was slow, it did occur over extended periods of time. Thus, as Fig. 11 shows, after 100 hr at operating potential in air, the initial current upon introduction of 100 ppm CO in air was higher but then decayed to a lower level.

In general, the measured CO oxidation current continued to decrease with time. The rate of this decrease diminished with increasing time of operation. This behavior is graphically shown in Fig. 12. After approximately 30 days of operation, the rate of current decrease reached a level of 1 to 2% per day (24 hr).

Experiments were also carried out to investigate procedures for electrode reactivation. Temporary polarization of the sensing electrode to potential values cathodic of 0.4 V versus RHE resulted in an increased CO oxidation current (see Fig. 13). The current value, for example, 15 hr after cathodic stripping was, however, not as high as the new electrode after the same time interval.

For the electrode TFE 40/20 II shown in Fig. 13, the detection current for 50 ppm CO after the first of 15 hr of continuous operation was 45 μA and decayed at a rate of about 4% per 10 hr. Eventually, after about two months of operation under various conditions, the electrode reached a detection current of approximately 20 μA for a 50 ppm CO in air mixture As Fig. 13 shows, after continuous sampling for 15 hr succeeding the cathodic polarization, the current value was 36 μA and the rate of decay approximately 8% per 10 hr. This behavior was found to be typical and leads

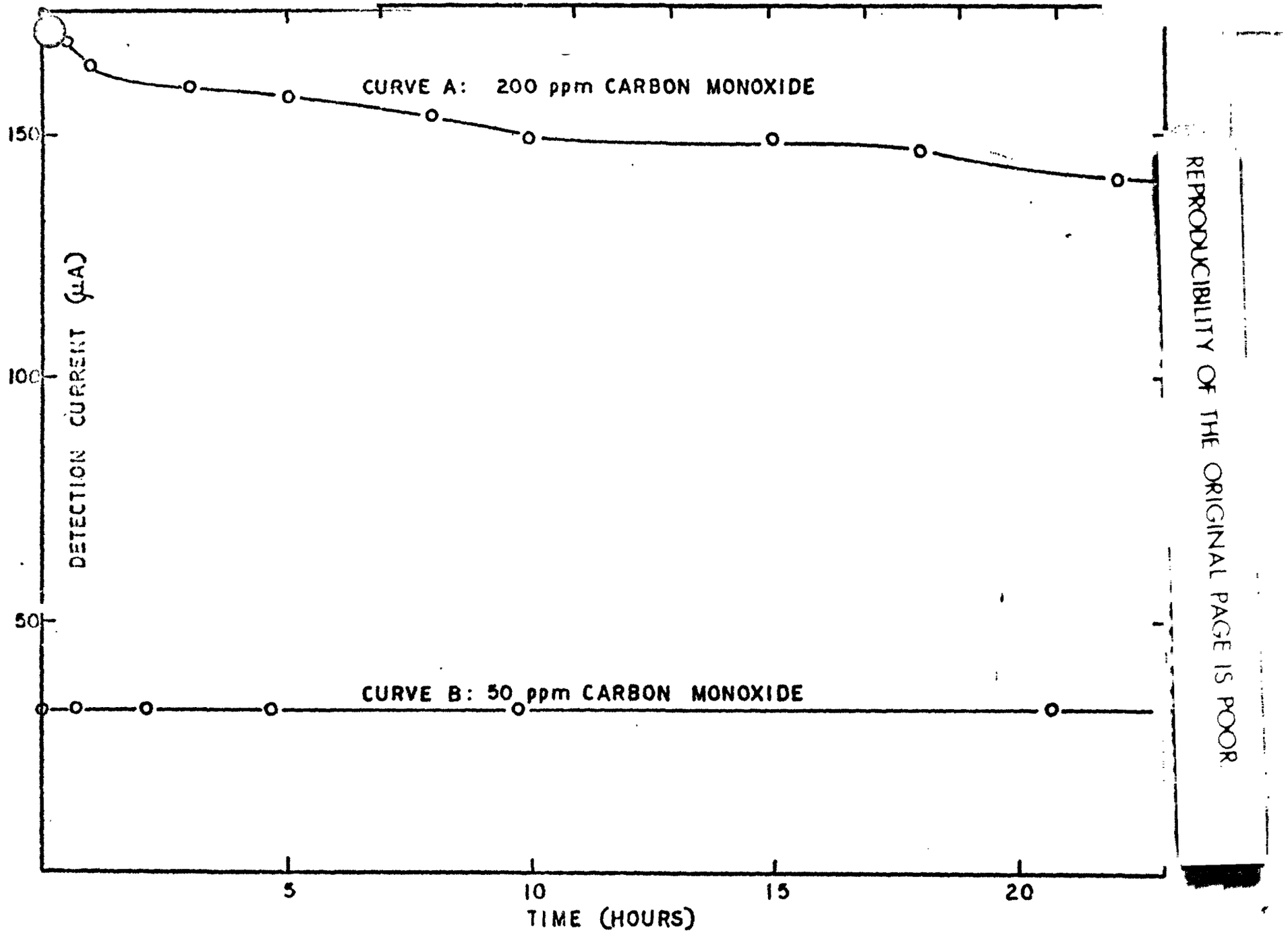

Fig. 10. Detection current for 50 ppm carbon monoxide on an electrode previously exposed to 200 ppm CO

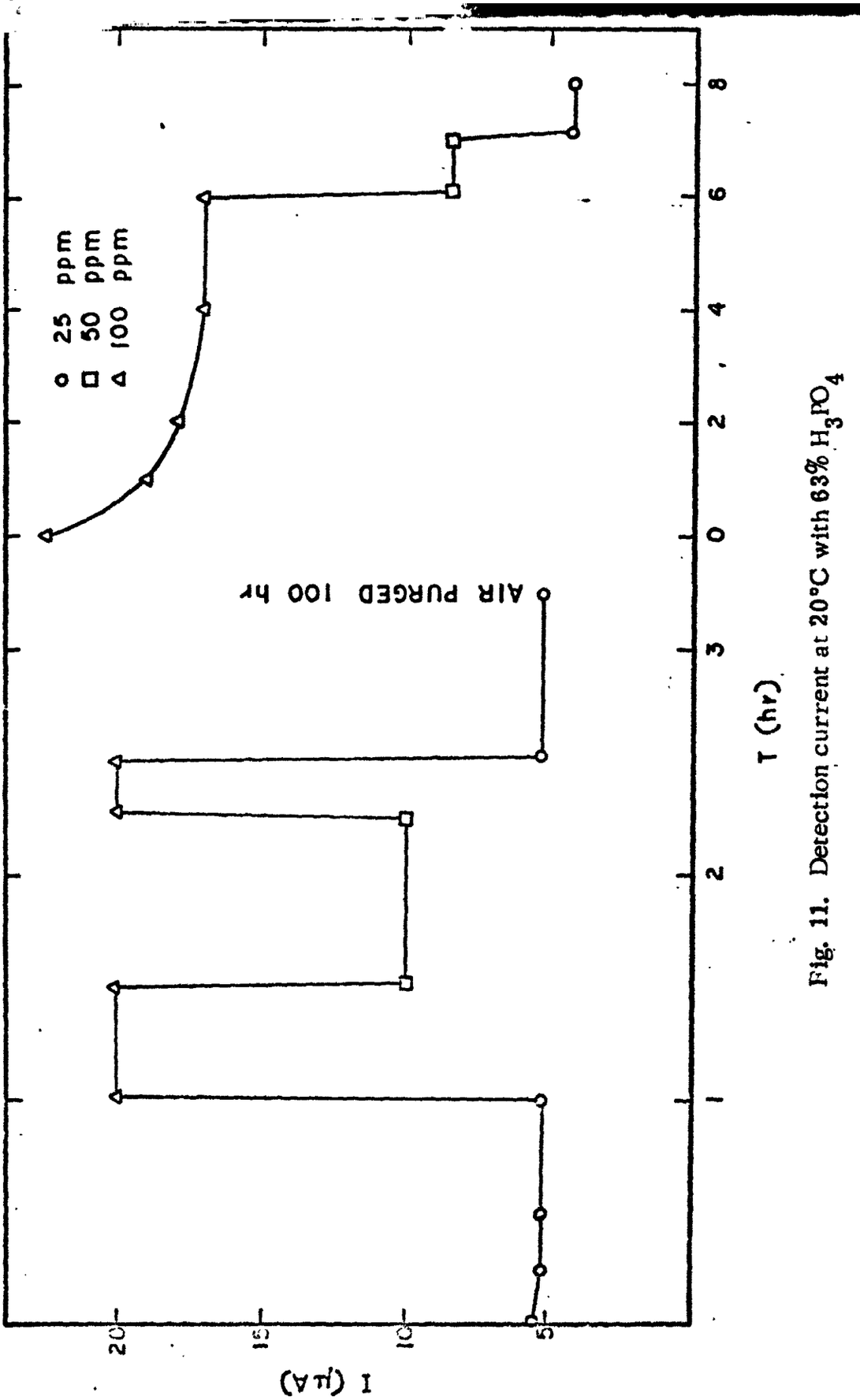

Fig. 11. Detection current at 20°C with 63% H_3PO_4

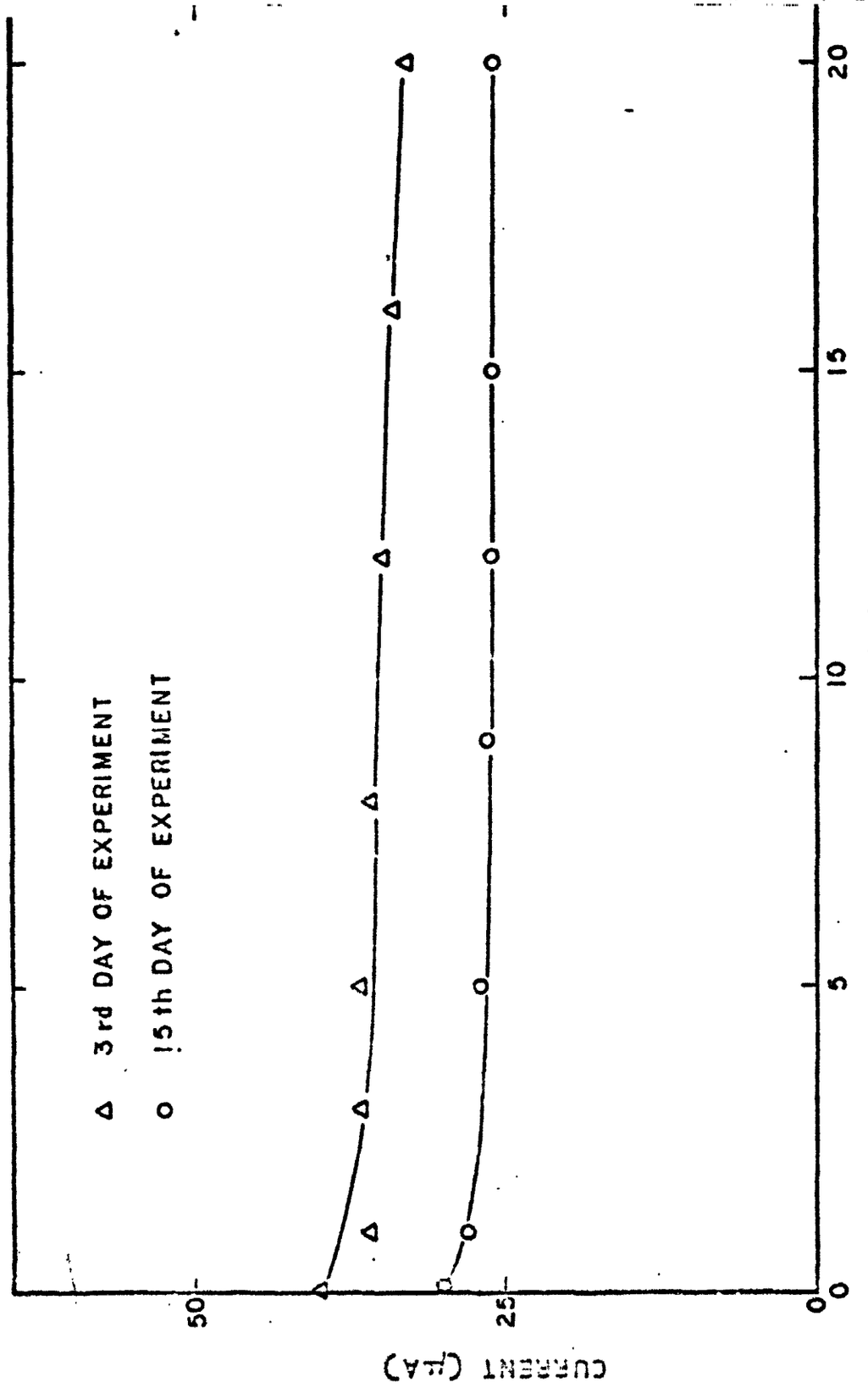

Fig. 12. Oxidation current for 50 ppm CO, electrode TPE 40/20 I, 21°C

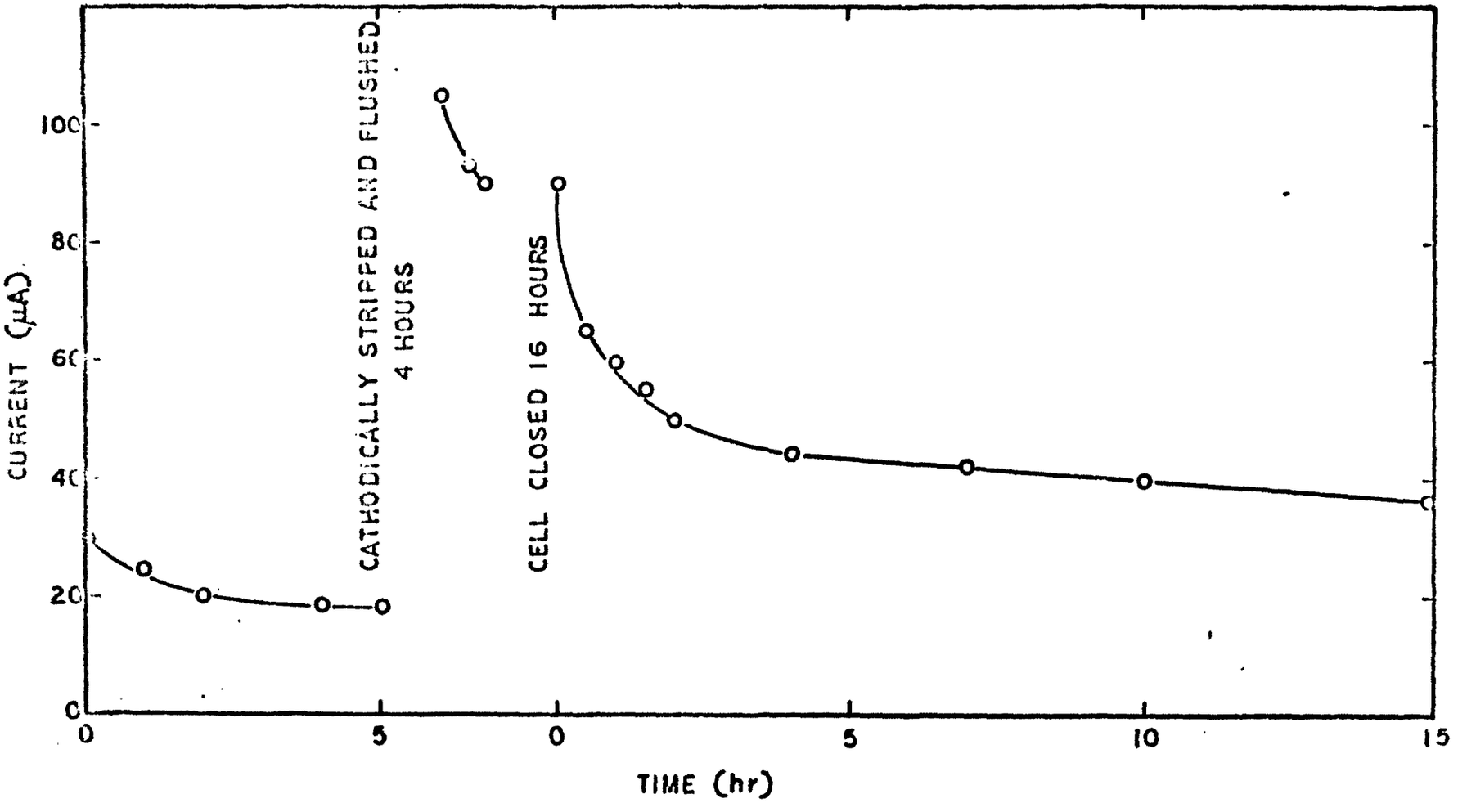

Fig. 13. Detection current for 50 ppm CO, electrode TFE 40/20 II, 21°C

to the conclusion that even though the oxide layer on the platinum surface can be removed by cathodic polarization, the complete desorption of the inhibiting species is not possible by this procedure. More successful, however, although not completely satisfactory, is a repeated anodic and cathodic polarization of the sensing electrode.

3. Effect of CO concentration

The current for the anodic oxidation of CO on the various Teflon-bonded platinum electrodes was found to be directly proportional to the CO concentration in the gas phase. Typical detection currents as a function of CO concentration for two different electrodes are shown in Figs. 14 and 15.

In some instances, the CO concentration in the gas phase was raised up to 1000 ppm, and only at these high concentrations were deviations from linearity observed. As discussed earlier, the detection signal at any given concentration did decline slowly with time upon continuous sampling. However, at any one time the linearity between CO concentration and detection current was maintained. This is also shown in Figs. 14 and 15.

4. Effect of electrode structure

In general, the electrode structure is of significant importance for the rate of the electrode reaction, and it may determine which part of the overall process is rate limiting. For our CO detector, we have employed Teflon-bonded platinum electrodes which consist of an interwoven network of hydrophilic, electrolyte-filled platinum black agglomerates and hydrophobic gas channels formed by the Teflon particles. Fig. 16 schematically shows the structure of a Teflon-bonded fuel cell electrode. The geometry and ratio of hydrophilic and hydrophobic pores in these electrode structures can be strongly influenced by the particle size and amount of both the Pt black and the Teflon as well as manufacturing and sintering conditions.[4]

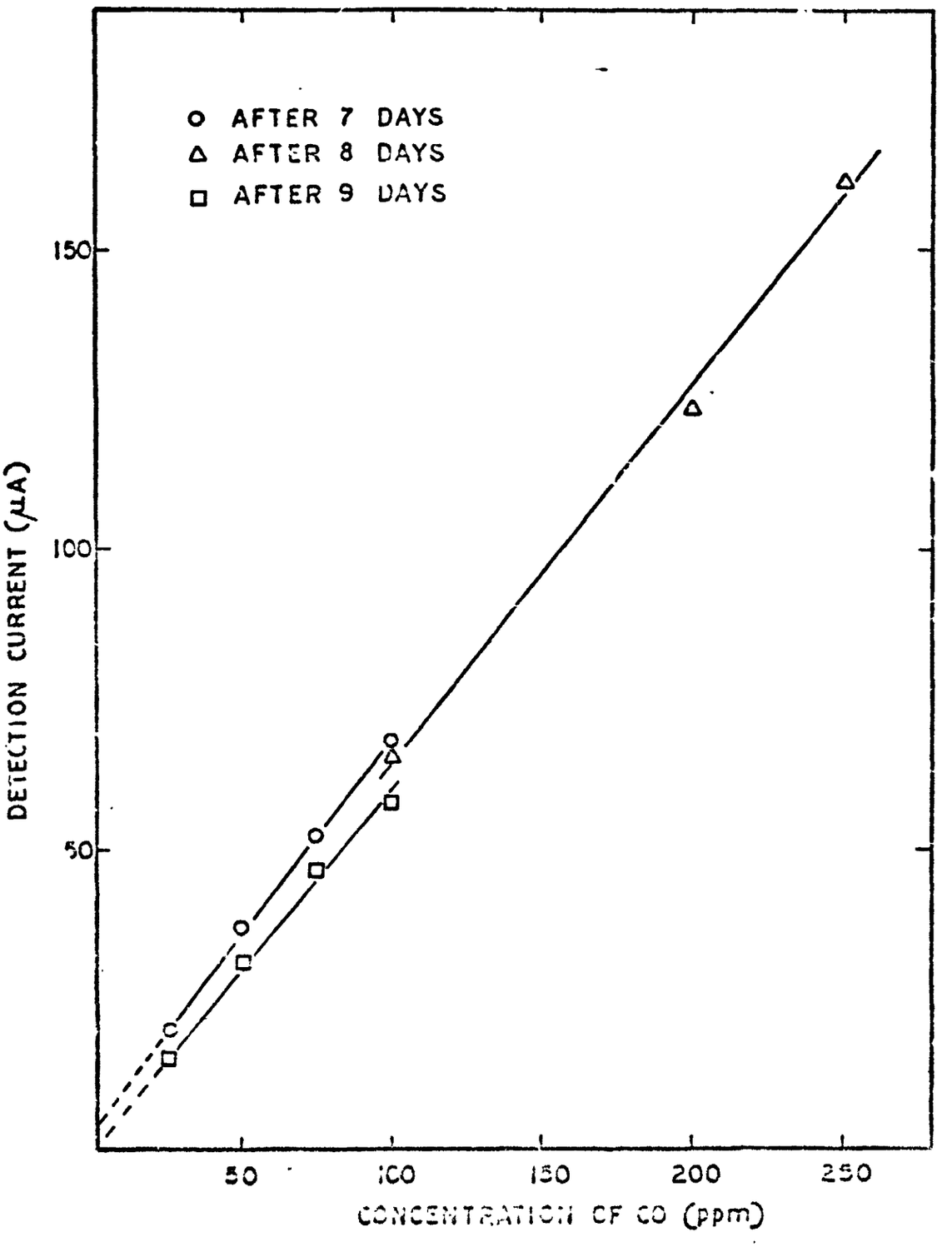

Fig. 14. Detection current versus concentration of CO for electrode [illegible] at 21°C.

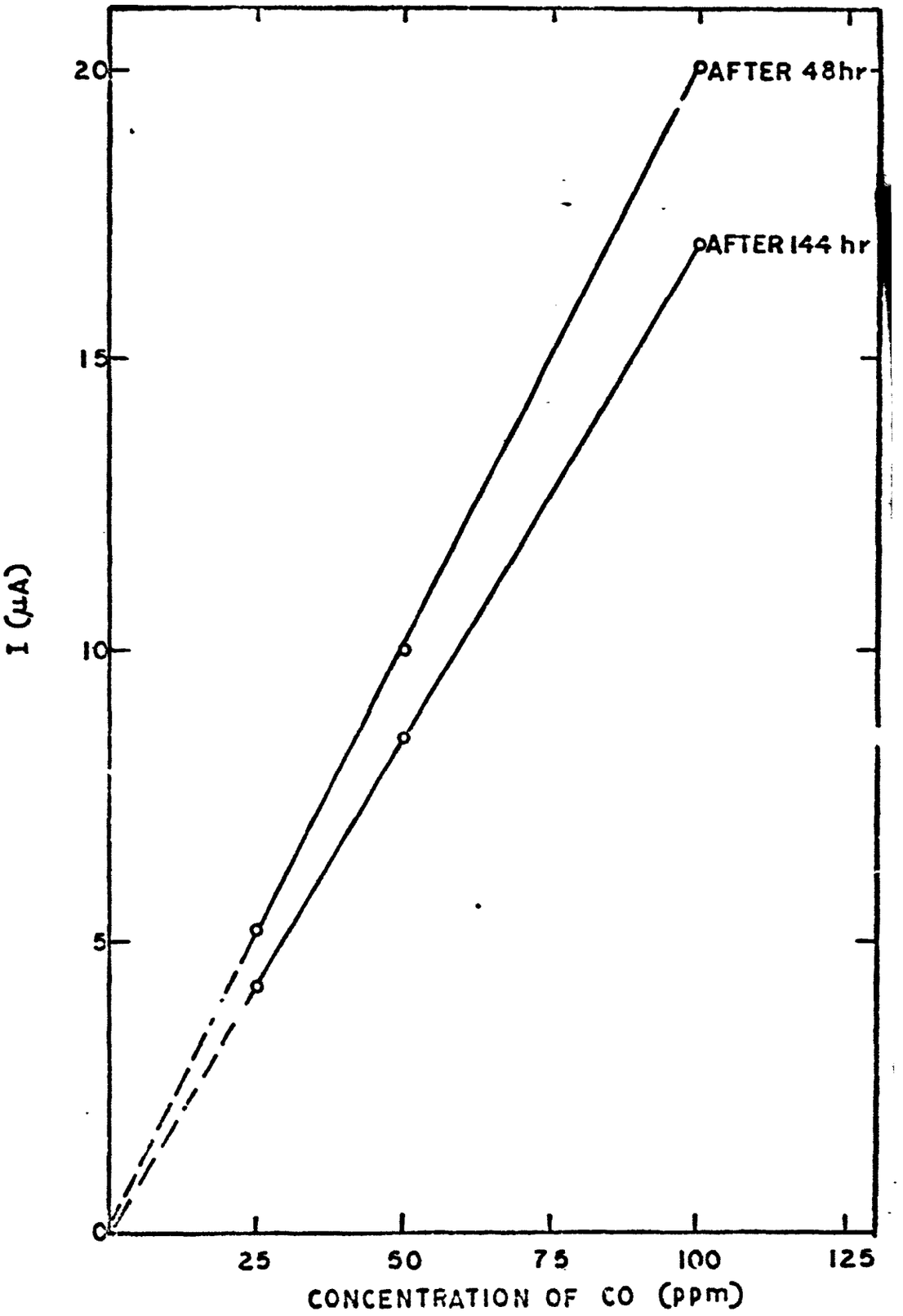

Fig. 15. Detection current versus concentration of CO, electrode Pt TFE 10/25. 20°C

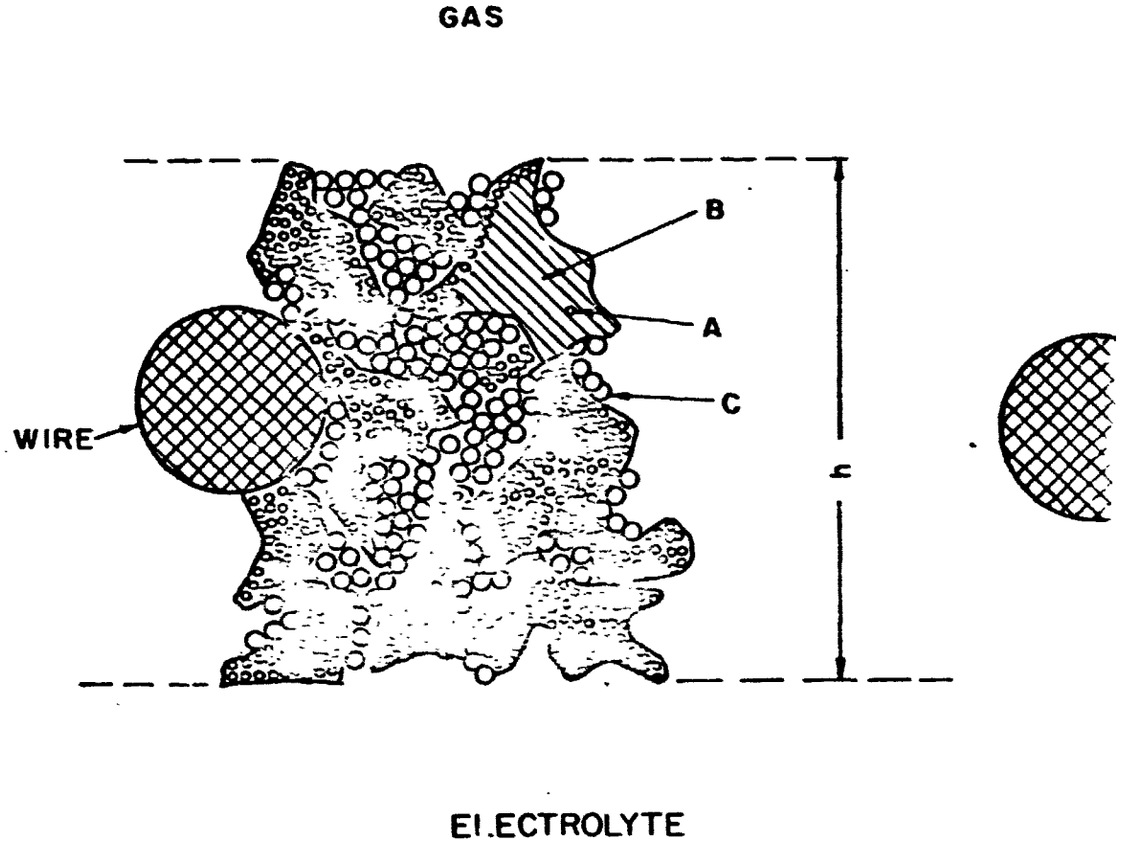

Fig. 16. Schematic representation of a hydrophobic porous electrode made of Teflon-bonded platinum black. (A) Catalyst particle; (B) Agglomerate; (C) Teflon particle

In order to find an optimum electrode with respect to signal stability and response time, we prepared and tested electrodes with 8 to 50 mg Pt/cm^2 and with a Teflon content of 15 to 30%. In addition, some electrodes contained a hydrophobic backing.

The results can be summarized as follows:

1. The CO oxidation current is approximately proportional to the platinum surface and thus for equivalent preparations proportional to the platinum loading.

2. The diffusion in the gas phase was not rate limiting under any condition investigated.

3. The rate of signal decay upon continuous CO sampling was practically independent of electrode structure.

4. The response time was longest with the highly loaded low Teflon electrode (Pt TFE 50/15).

5. The Teflon content and the hydrophobic porous Teflon backing appeared not be have any influence on the CO oxidation current as such. However, both parameters strongly affected the wetting characteristics of the electrodes and thus their sensitivity to drying or flooding. The electrolyte balance, especially the amount of electrolyte in the electrode structure, had a strong effect on the CO detection current. The electrolyte concentration between 50 and 65% H_3PO_4 was of practically no effect.

The best results with respect to response time and wetting characteristics were obtained with electrodes of approximately 10 to 20 mg Pt/cm^2 and 25% Teflon with a thin hydrophobic backing.

5. Effect of temperature

The CO oxidation current at a given electrode is strongly dependent on operating temperature. Fig. 17 shows results obtained at two CO concentrations in an Arrhenius diagram. The measurements were conducted in the sequence 35°, 50°, 20°, 35°C. The repeat value at 35°C after a test period of six days at various temperatures was approximately 15% lower than the original current and is a reflection of the slow continuous signal decrease with time. The data in Fig. 17 follows a good straight line. From the slope:

$$\frac{d\,(I)}{d\,(1/T)} = -\frac{E}{R} \qquad (9)$$

an activation energy of 6.5 kcal/mole was obtained. This relatively high activation energy, compared to a value of 3 to 4 kcal/mole which one might expect for a diffusion-controlled reaction. is a further indication that we are. in fact, not dealing with a purely diffusion-controlled process.

The data showed also that there is no principle advantage in operating the CO sensor at elevated temperature. (There are practical reasons for the final design to operate at the environmental temperature of the space capsule.)

C. Results in Sulfuric Acid Electrolyte

1. Effect of potential and time of operation

The oxidation of CO in sulfuric acid electrolyte has much in common with the previously discussed CO oxidation in phosphoric acid. There are, however, significant differences, and these will be specifically elucidated in the following paragraphs.

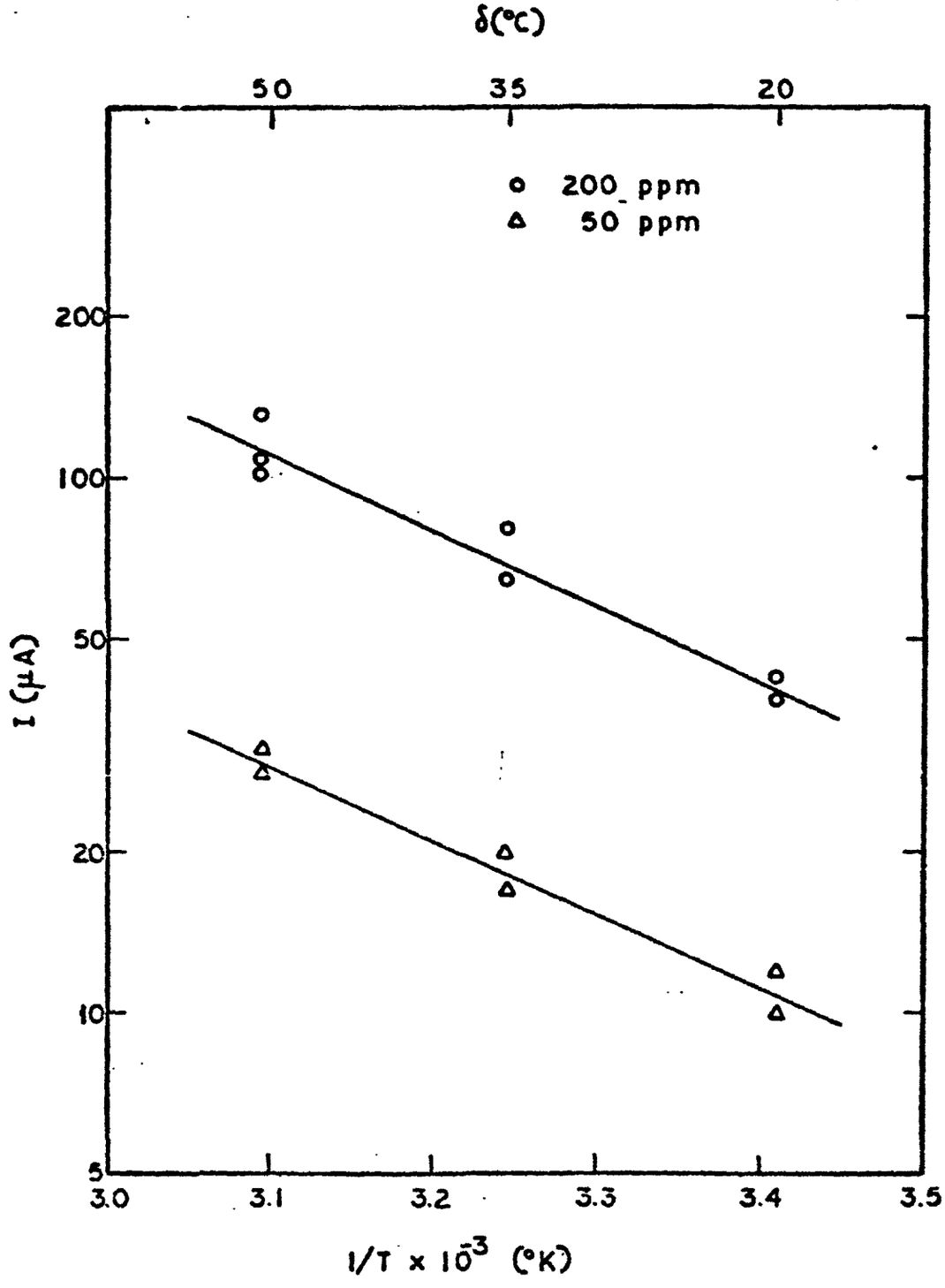

Fig. 17. Temperature dependence of the CO oxidation current (Electrode Pt TFE 40/20 at 1.2 V versus RHE, 63% phosphoric acid electrolyte)

A comparison of the CO detection current at the same electrode material in the two electrolytes is shown in Fig. 18. In both cases, the electrode potential is 1.2 V versus RHE and both electrodes have been operating for extended time under various conditions prior to the run shown. The most obvious difference is the detection current, which was considerably higher in the sulfuric acid electrolyte. The rate of current decay as a function of time, however, is surprisingly similar in both cases, with approximately 2 to 3% per day of continuous sampling.

The partial CO oxidation current recovery upon stand in air and the subsequent decay transients observed in phosphoric acid were not found in the sulfuric acid electrolyte.

In a search for operating conditions which could result in a more stable CO oxidation current with time, electrode pretreatment with high CO concentrations, an increased surface oxide deposition by pre-equilibration at more anodic potentials, and the variation of the operating potential were investigated. An electrode at 1.2 V versus RHE showing a practically steady CO oxidation current (Fig. 19) was polarized to 1.55 V versus RHE for 20 min and then returned to 1.2 V versus RHE. During the following 2 hr of CO sampling, the detection current decreased from 88 to 73% of the value prior to the anodization. Subsequent cathodic stripping reactivated the electrode, but not to the state of the new electrode. Upon exposure to CO, the detection currents decreased again relatively rapidly to the original value. Fig. 20 shows an electrode which was reactivated by two anodic-cathodic cycles to remove oxidizable and reducible species and then treated with 10% CO for 35 min. During the following CO sample, detection currents were practically identical to those observed previous to this treatment. The initial current was probably due to the slow equilibration of the surface oxide layer after its cathodic

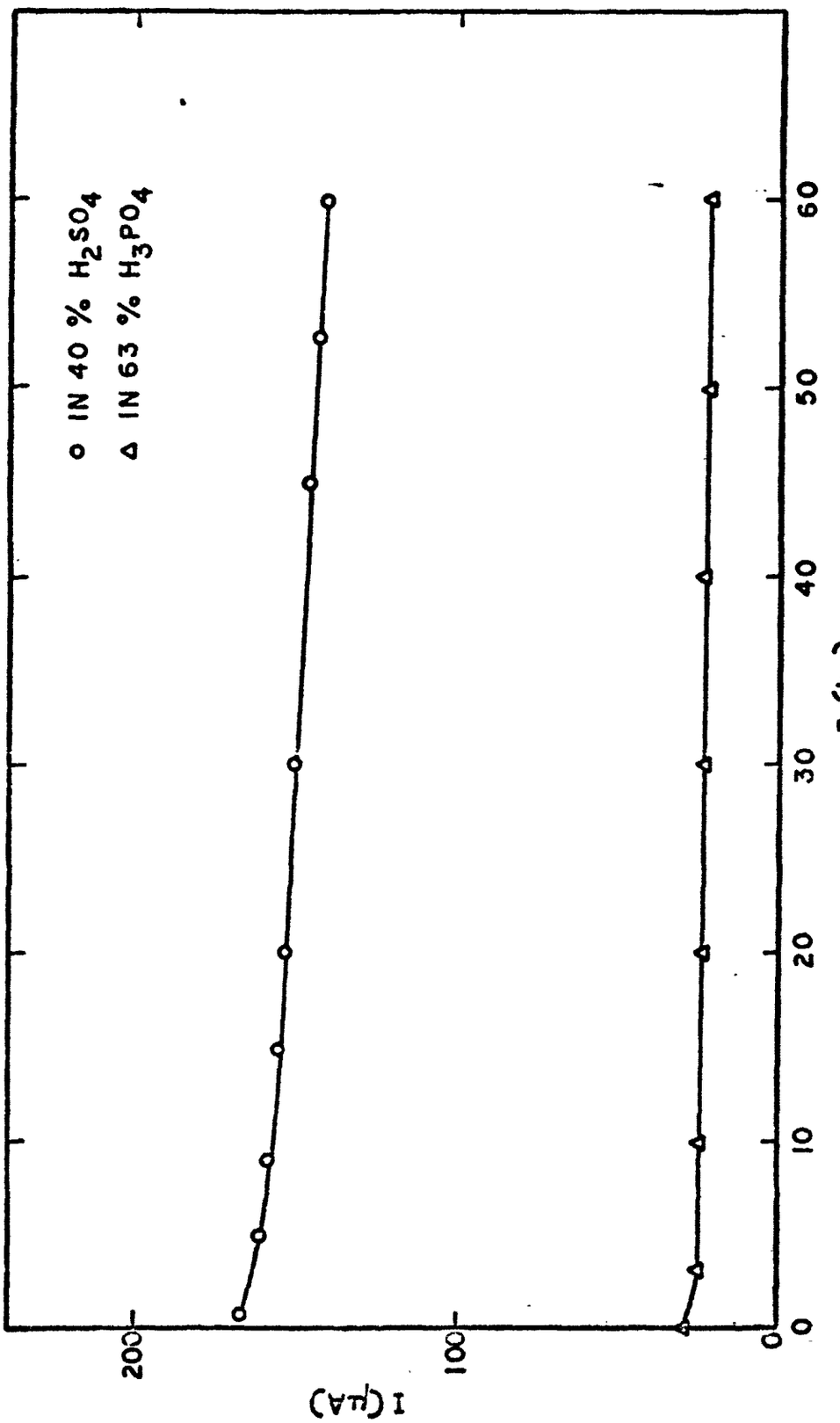

Fig. 18. Detection current for 50 ppm CO, electrode Pt TFE 40/20, 21°C

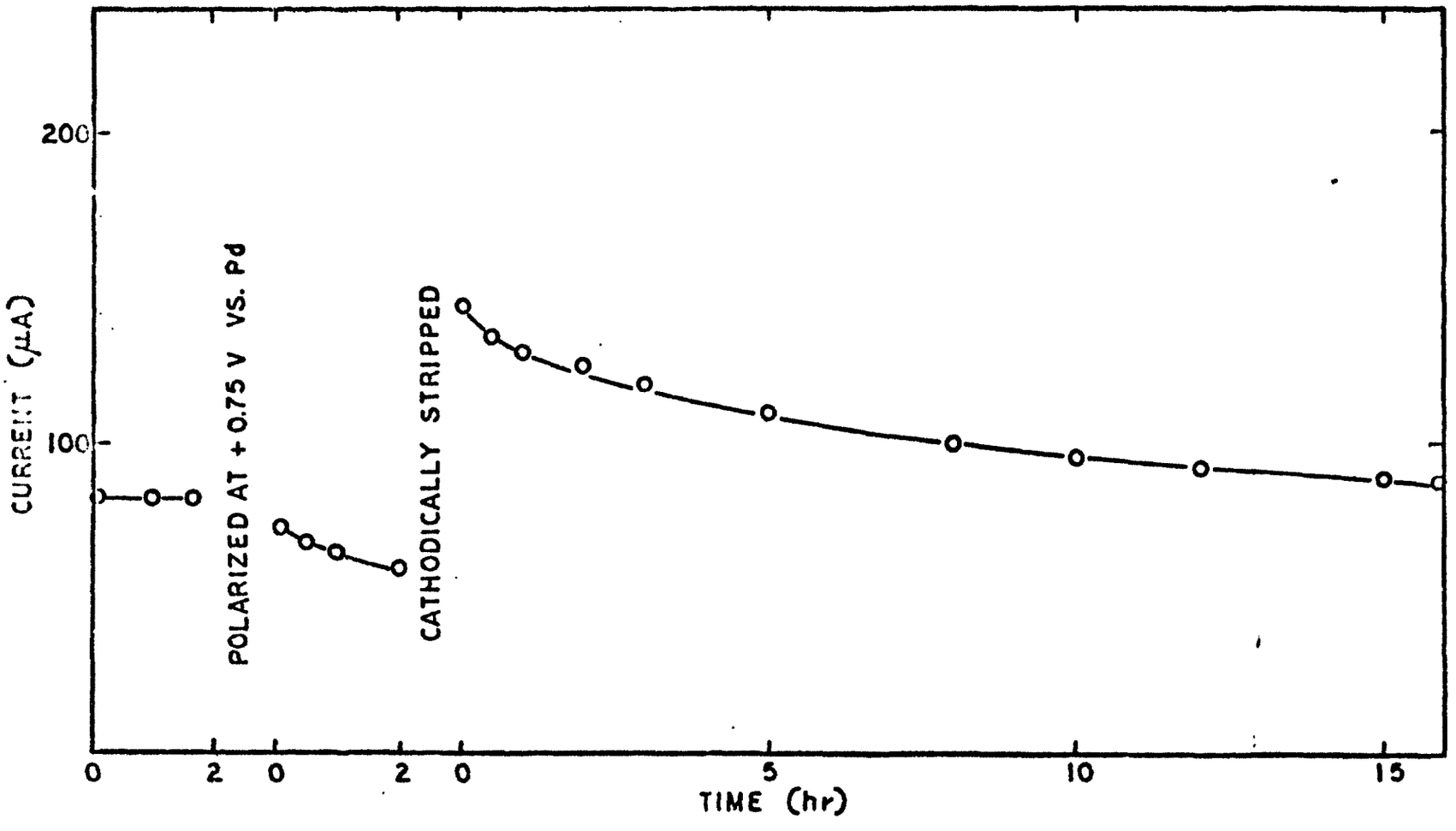

Fig. 19. Detection current for 50 ppm CO, electrode TFE 40/20 III at +0.4 V versus Pd

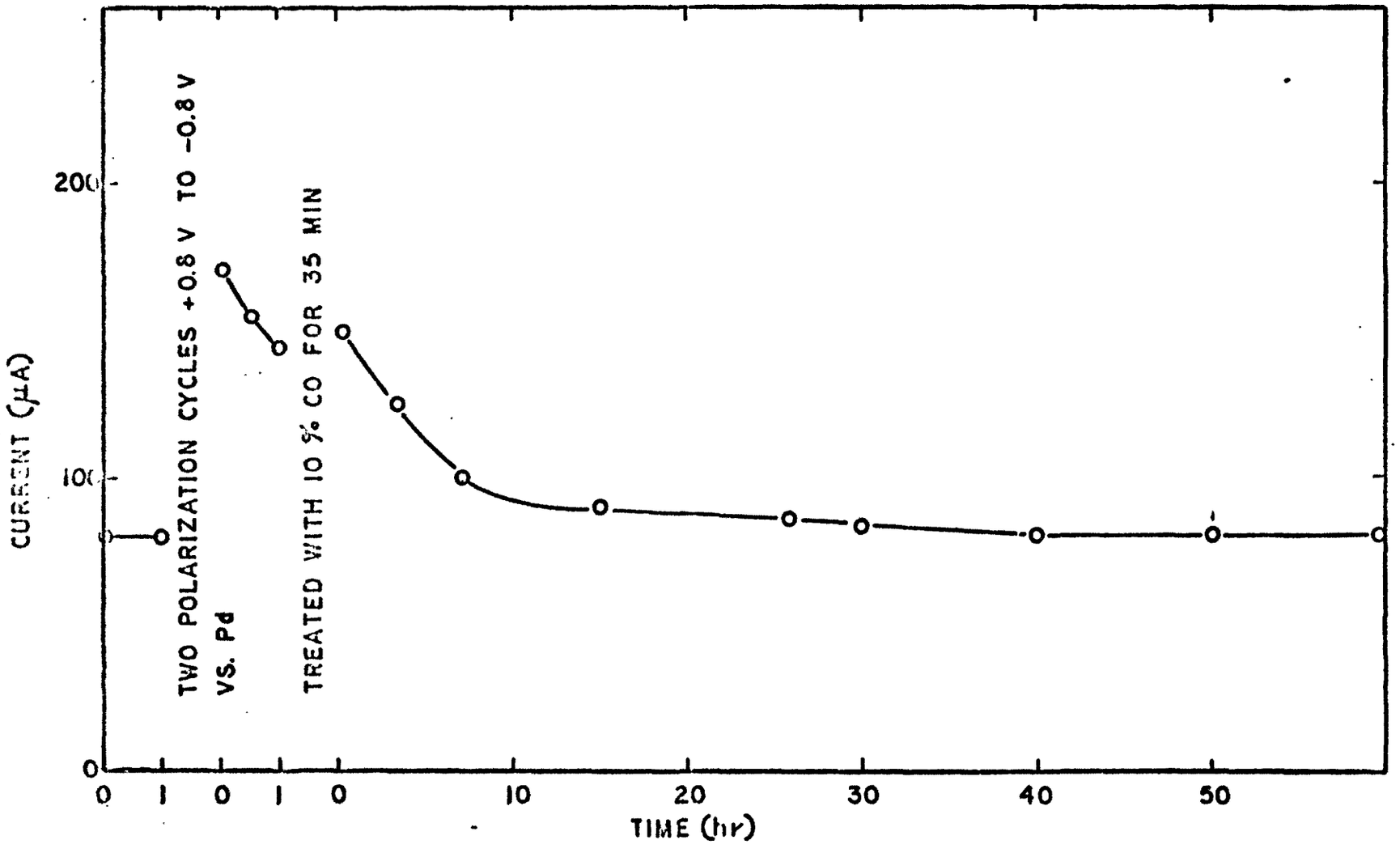

Fig. 20. Detection current for 50 ppm CO for electrode TPE 40 20 III at +0.4 V versus Pd

removal. The current signals during the treatment with 10% CO in air before and after the 60-hr experiment were very similar (see Fig. 20). The initial current value was approximately that which one would expect by linear extrapolation of the low current data. At this high CO concentration, however, the detection current decayed relatively rapidly.

The variation of the working electrode operating potential had a significant effect on the CO detection current. Fig. 21 shows the measured current upon stepping up of the electrode potential. The current transients were mainly due to the buildup of the surface oxide layer. Even though steady-state had not been achieved at the higher potentials during the time of this experiment, it can be seen that a maximum CO detection current was obtained at potentials of 1.05 to 1.075 V versus RHE. More important than the maximum CO oxidation current was, however, the observation that the rate of long-term current decay was also a function of operating potential. At 1.0 V versus RHE, for example, practically no current decay could be detected. Fig. 22 shows actual measurements (continuous CO sampling) with a detector operated at 1 V versus RHE. (The slight variation appeared to be due to inaccuracy of the gas mixer.).

At higher electrode potentials, a slow change in the electrode surface activity for CO oxidation with time (several hours to days) was observed and in the absence of CO is probably due to a slow increase in the thickness or change in the structure of the adsorbed oxygen layer. Thus, in order to have the CO detector operational (within calibration), the sensing electrode would have to be kept at a set potential at all times.

When operating in the low potential region (~1 V versus RHE), where we operate at lower oxygen coverage and in a range where the oxygen adsorption and desorption is more reversible, this may not be necessary. In fact,

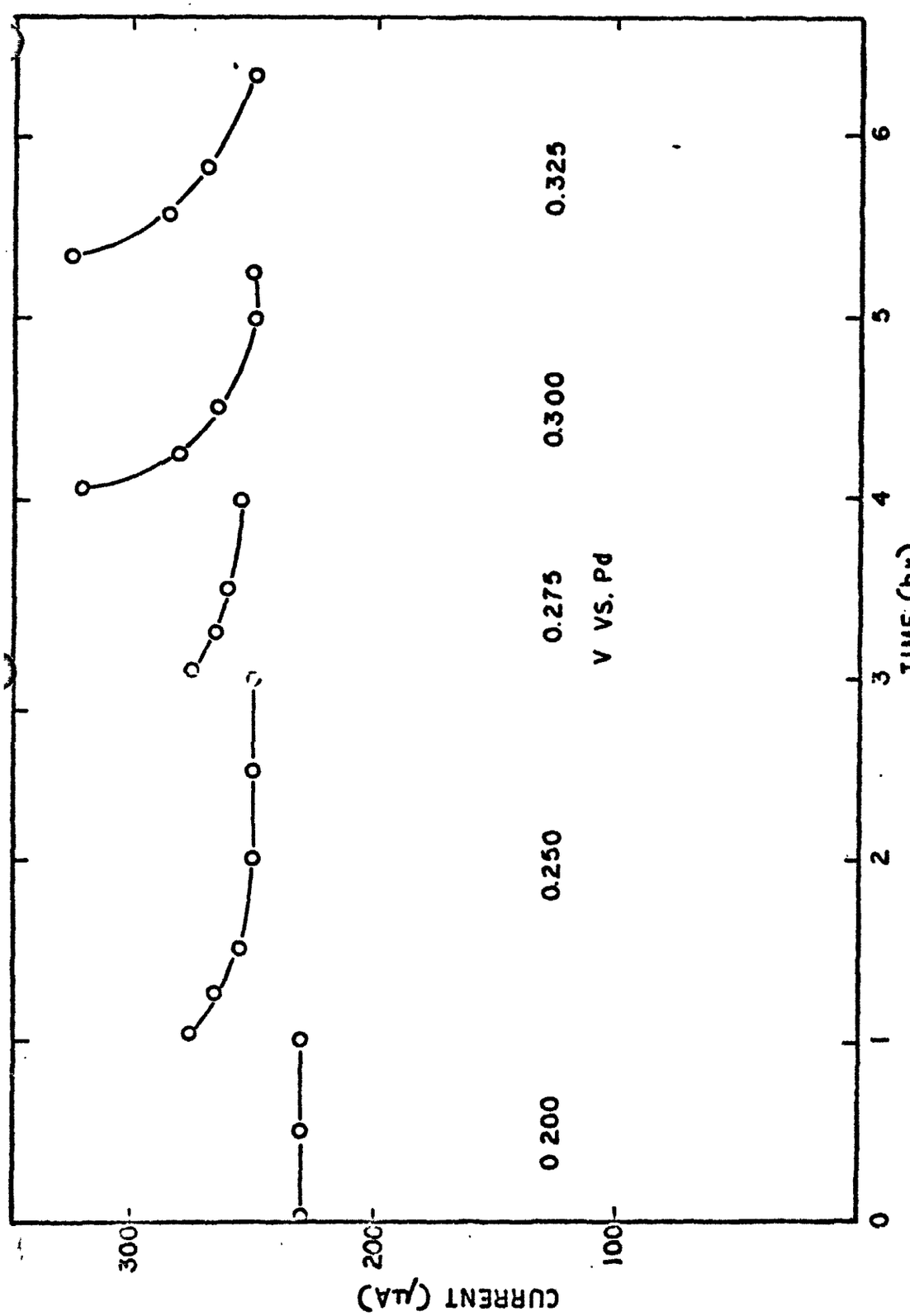

Fig. 21. Detection current for 50 ppm for electrode TFE 20/20 I

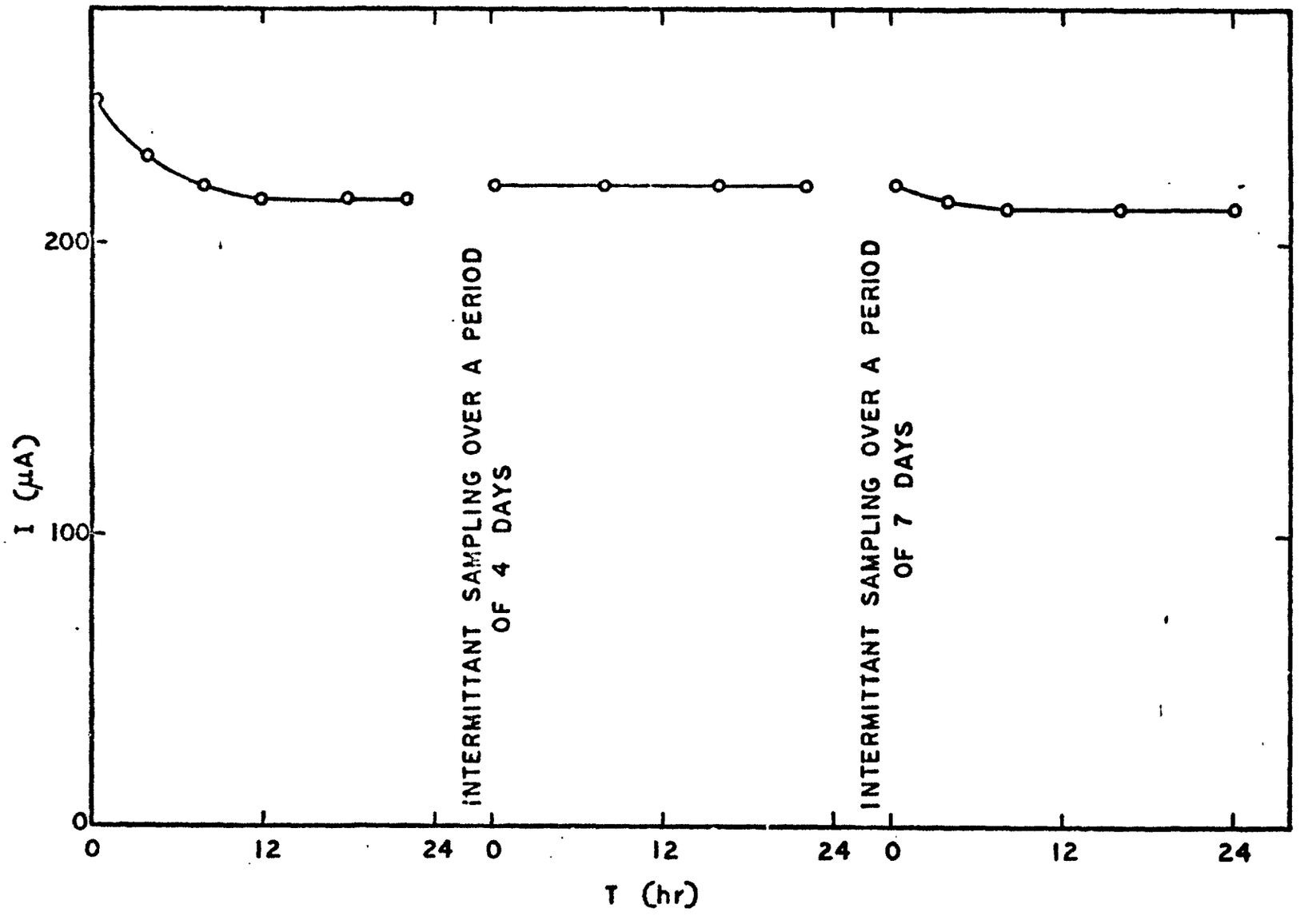

Fig. 22. Detection current for 50 ppm at 1.0 V versus RHE

we have carried out experiments to this effect which showed that the cell can be left at open circuit. After CO sampling, followed by air flushing and open circuiting, the electrode potential decreased to approximately 950 V versus RHE. Upon return to potentiostatic control (1 V versus RHE) after extended stand (60 hr), only 60 sec were required to obtain background currents of less than 10 μA, and after 60 sec, stable and reproducible readings were obtained.

2. Effect of operating temperature

The CO detection currents obtained in sulfuric acid electrolyte at various temperatures are shown in Fig. 23. The data presented for two operating potentials exhibit good linearity in an Arrhenius diagram. The activation energies for the overall reaction were determined to E = 4.0 kcal/mole at 1.2 V versus RHE and E = 2.6 kcal/mole at 1.0 V versus RHE. This compares to a value of E = 6.3 kcal/mole for the oxidation of CO in phosphoric acid electrolyte. It is interesting to note the difference in the energy of activation as a function of electrode potential, indicating a change in the nature of rate controlling step and not only a change in effective surface area.

3. Effect of fluctuations in water vapor pressure

In order to establish if a gas prehumidification would be required for reliable operation of the CO detector in the space capsule, it was necessary to test the sensitivity of the detector to fluctuations in water vapor pressure within the range of 8 to 12 mm Hg (the approximate limits for the capsule environment). Prehumidification will, of course, be necessary for operation of the CO detectors in an uncontrolled terrestrial environment or during test operation with "dry" gas from high pressure tanks.

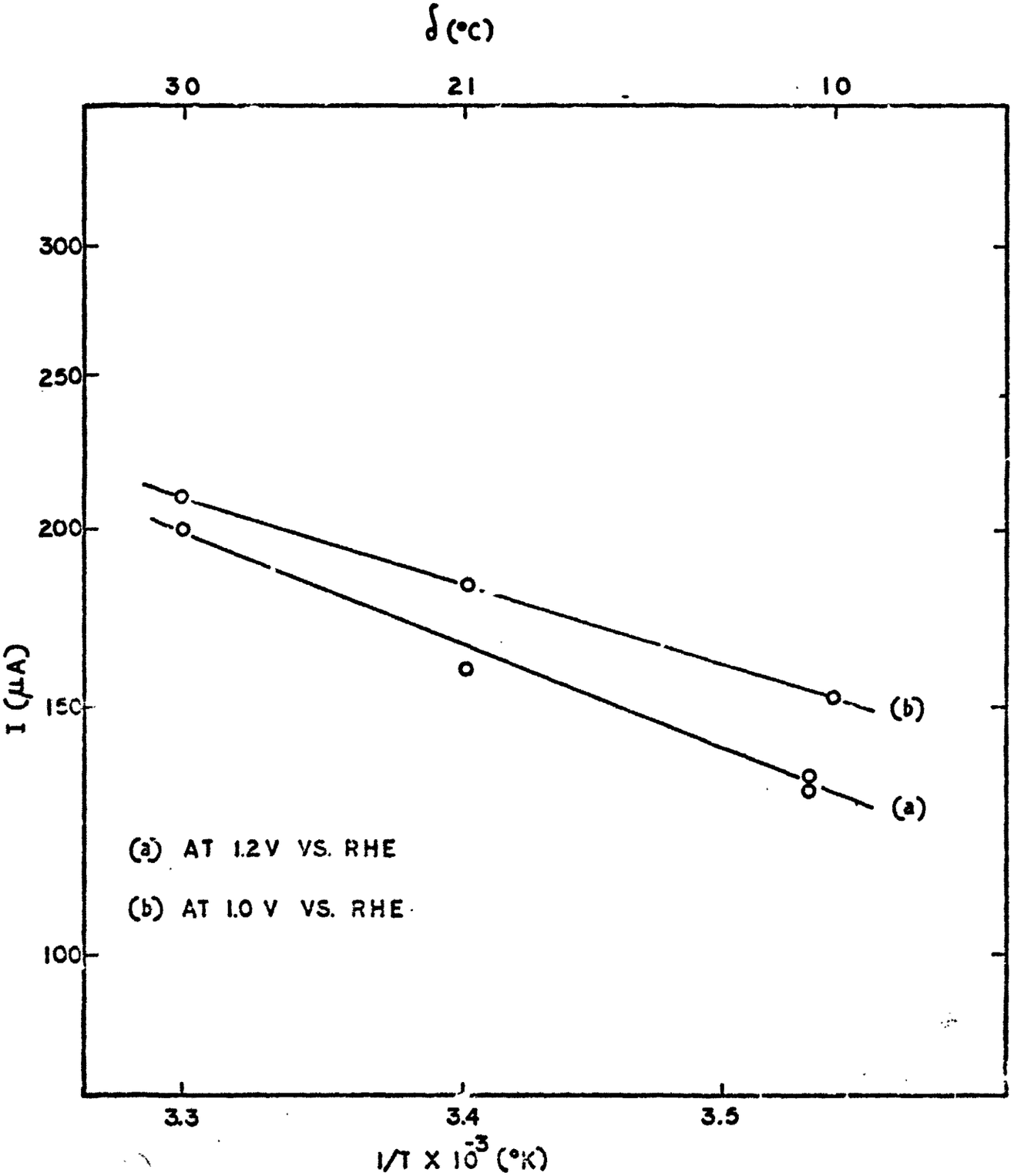

Fig. 23. Temperature dependence of the CO oxidation current for electrode TPE 40 20 II in 40% H_2SO_4

Both the short-term as well as the long-term effects were investigated. The effect of changing from the standard condition of 10.5-mm to 8-mm water vapor partial pressure in the CO containing air was a slow 2 to 5% decrease in signal over a 10-hr period of continuous flushing with the drier gas. Further flushing at the same vapor pressure up to 65 hr did not result in any additional decrease in current. When the gas was then directed through the 10.5-mm presaturator, a period of 20 min was required for the signal current to return to its original value. The cell was also cycled between 10.5 and 12-mm with 60 to 90 min at each vapor pressure. There were no changes in detection current which were in excess of 1% and therefore exceeded experimental error. Upon operation at a H_2O partial pressure of 12-mm for 16 hr with continuous flushing of 50 ppm CO, there was no detectable change in current. These experiments show that the signal current is relatively independent of fluctuations in vapor pressure over the range of 8 to 12 mm Hg. The decrease in current observed with the lower humidity gas is completely reversible and can be further reduced by increasing the amount of electrolyte in the matrix of the cell. The effect of changes in gas humidity is twofold: (1) with changing electrolyte concentration, the viscosity changes, and (2) the electrolyte volume changes. Rapid humidity changes can cause concentration changes in the pores of the electrode without significantly affecting the bulk of the electrolyte. Over longer times, the change in electrolyte volume is more significant.

For example, at a relative humidity of 80% (vapor pressure = 15 torr), the cell electrolyte at 21°C would achieve an equilibrium concentration of 20%, and then the electrolyte volume would double. The corresponding decrease in relative viscosity would be from 2.68 to 1.54 centipoise. Ultimately, at a sufficiently high vapor pressure, the cell would become flooded and no longer be operative.

D. Conclusions

From the experimental results discussed in the preceding sections, we can draw the following conclusions pertinent to the construction of a practical electrochemical CO monitor:

1. The presence of air limits the potential of operation to between approximately 1.0 and 1.4 V versus RHE. In phosphoric acid, the CO oxidation current on Teflon-bonded platinum electrodes is practically independent of potential within this range. However, the current is not diffusion controlled and it decays with time. At least two mechanisms are responsible for this decline in signal: (a) a slow increase and/or rearrangement of the oxide on the electrode surface, and (b) a slow accumulation of an intermediate of a side reaction which acts as an electrode "poison." The temperature dependence of the CO oxidation follows an Arrhenius equation with an activation energy of 6.5 kcal/mole.

2. The oxidation of CO in a sulfuric acid electrolyte shows significant differences: the current is higher than with H_3PO_4 and is potential dependent. The rate of current decrease during continuous CO sampling also is a function of operating potential. A stable detection current is obtained in the lower potential region (~ 1.0 V versus RHE), while at higher potentials the signal declines. The activation energy of the CO oxidation in sulfuric acid was determined as 4 kcal/mole at 1.2 V and 2.6 kcal/mole at 1.0 V versus RHE.

3. The CO oxidation current was found to be fairly insensitive to variation in electrolyte concentration. However, the electrolyte level, and thus the humidity of the gas sample, have to be suitably controlled to prevent drying or flooding of the electrode. A special cell design has been developed which can tolerate appreciable humidity variations without effect on the CO detection current. This eliminates the need for special humidity controls in a space capsule environment, where the humidity can vary between 8 and 12 torr H_2O vapor and reduces the humidity control requirements for terrestrial use.

V. PROTOTYPE CARBON MONOXIDE DETECTOR

A. Instrument Design

1. General construction

A bench prototype carbon monoxide detector was built with the purpose of demonstrating its performance under practical conditions. The instrument was designed for test operation with compressed air-CO mixtures. It therefore does not contain a gas pump. (In an actual space capsule, the electrochemical cell, due to its particular design, could be mounted directly in the return gas duct of the air purification system.) The prototype was adjusted for a range of 0 to 60 ppm CO. Further, since remote monitoring was desired, no indicating instrument was mounted into the instrument case. An outside view of the instrument is shown in Fig. 24. In the development of the electrochemical cell, the heart of the sensing instrument, special consideration was given to space capsule conditions and environment. The hardware, however, does not constitute flight hardware.

A flow schematic of the prototype CO detector is shown in Fig. 25. In the following paragraphs, the major components are discussed in more detail.

2. Detector cell

The prototype CO detector contains as a sensing element an electrochemical cell as described in paragraph D and in Fig. 6. The sensing electrode consisted of Teflon-bonded platinum with 20 mg/cm^2 Pt and 20% Teflon on a tantalum screen support. The electrolyte was 40 wt % sulfuric acid. (This concentration has a water vapor pressure of 10 torr at 20°C equal to the mean value expected in the space capsule under normal operation.)

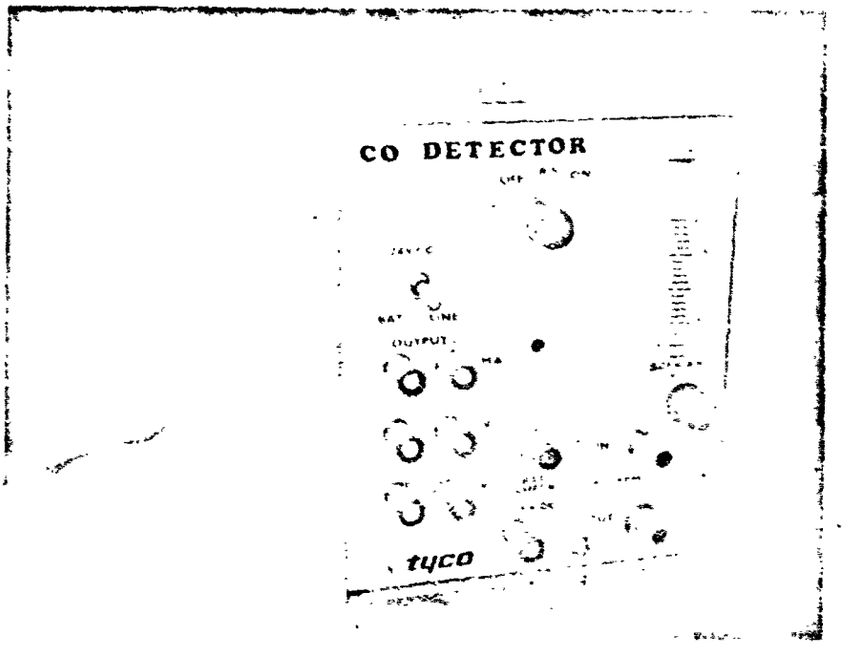

Fig. 24. Outside view of detector

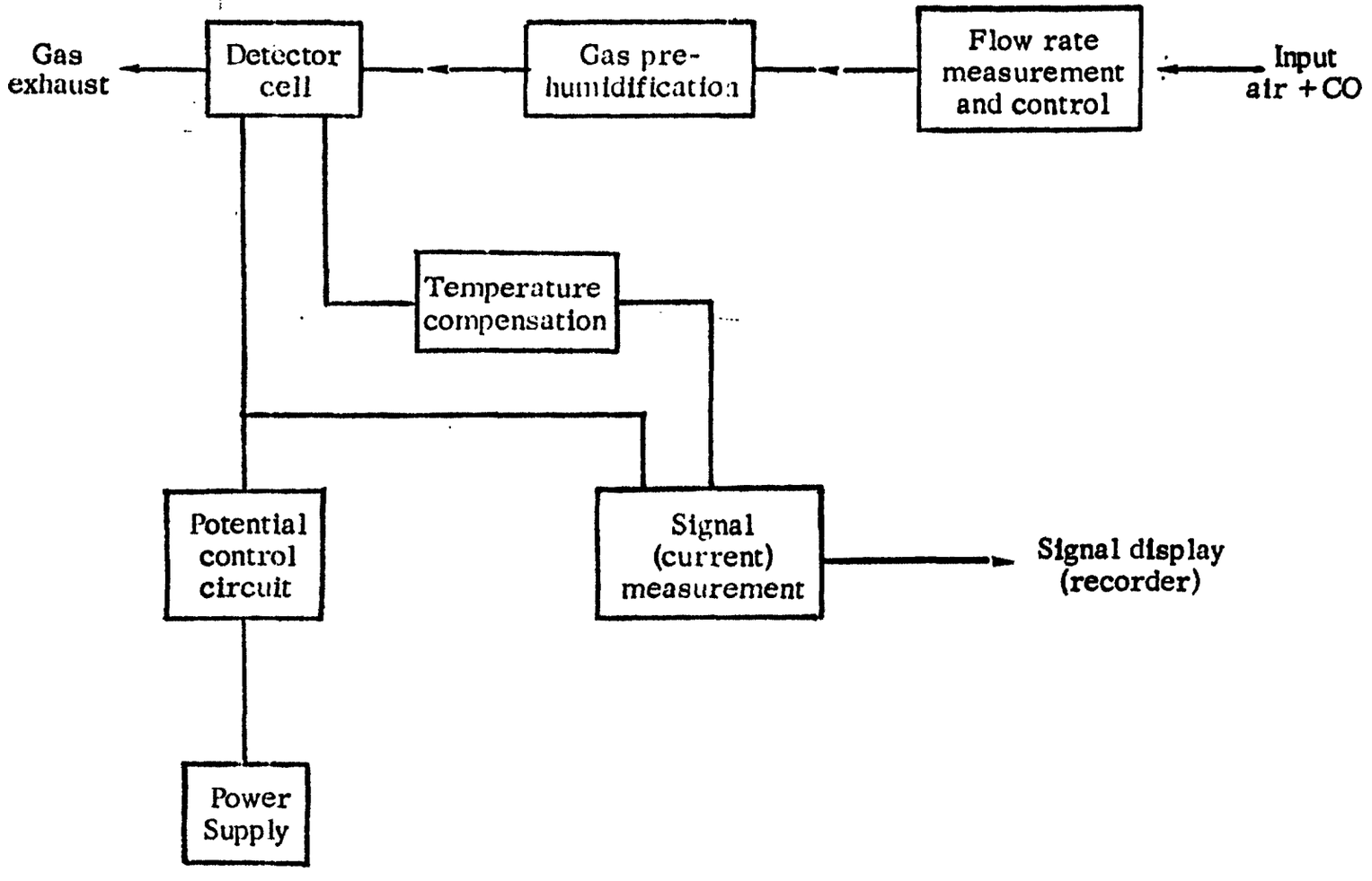

Fig. 25. Flow schematic of prototype CO detector

3. Presaturator system

Even though our cell is designed to operate without additional humidity control in the space capsule, a gas prehumidification is necessary when operating on dry cylinder gas. The prototype instrument contains, therefore, two presaturators (200 ml polyethylene bottles) in series, as shown in Fig. 26.

In the first bottle, the dry gas passes over approximately 50 cm^2 of pure water. It was determined that at flow rates between 1 and 2 SCF/hr, dry air would be humidified to approximately 10 torr water vapor pressure in this arrangement. Also, the bottle provides a large supply of water at a constantly exposed cross section, allowing long-term continuous testing (in excess of 1 mo) without necessity of refilling the H_2O presaturator. The function of the H_2SO_4 bottle is to further smooth out humidity fluctuations in either direction of the equilibrium value. It has a porous inner side wall (nonwoven polypropylene) to increase the gas liquid contact area.

4. Electronic circuit

a. Potentiostatic circuit

The potential of the sensing electrode is held at a predetermined constant value versus a Pd reference electrode by a potentiosatic circuit. This circuit is schematically shown in Fig. 27. It contains a high impedance input for the reference electrode. The control circuit delivers a maximum of ± 10 V and ± 1 mA. A more detailed circuit diagram is shown in Fig. 28. Special consideration was also given to the high capacity of the electrochemical cell, and in order to prevent potentiostat oscillation, a negative feedback to the control amplifier was provided. A protection circuit switches the cell to open circuit when the power supply voltage becomes

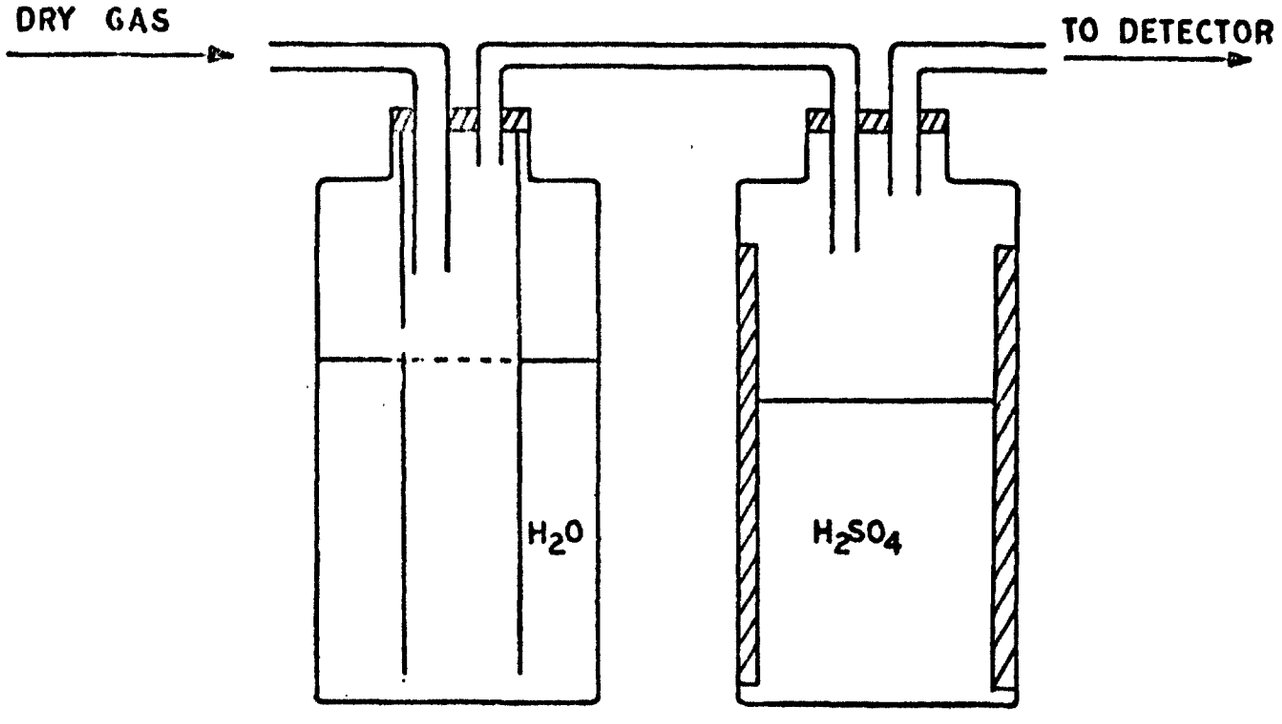

Fig. 26. Schematic of preliquidification arrangement

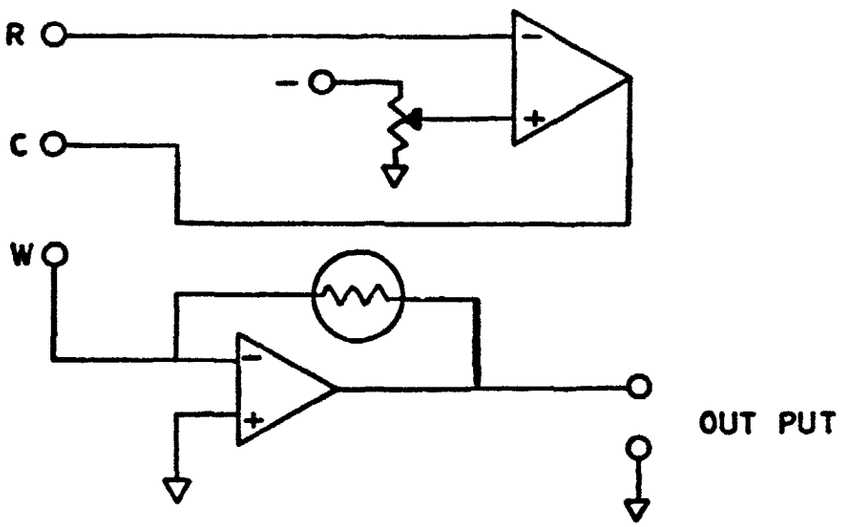

Fig. 27. Schematic of potentiostatic circuit

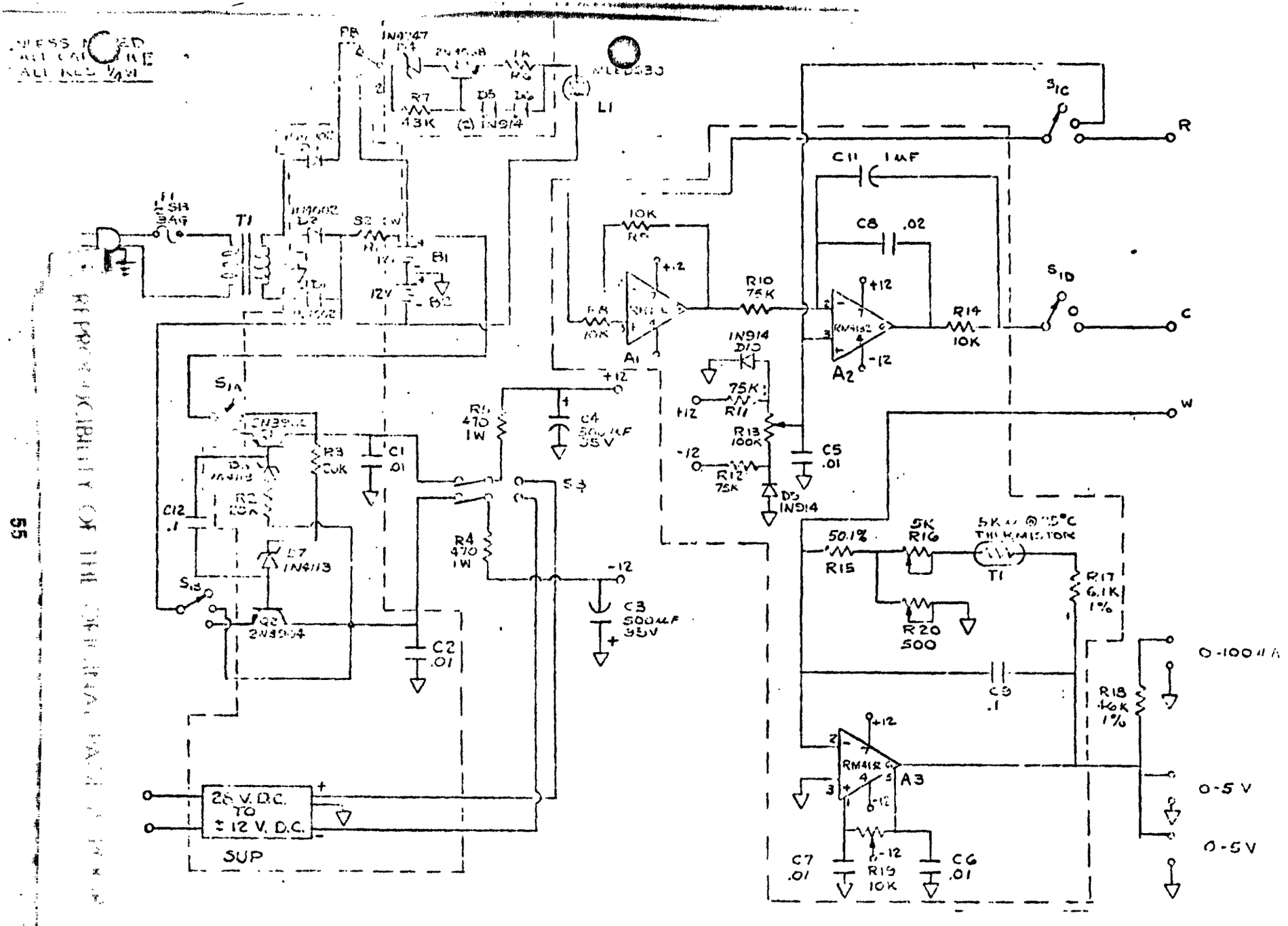

Fig. 28. Circuit diagram

insufficient. This prevents uncontrolled transients and protects the electrochemical sensor. This circuit has to be manually reset. All electronic components used are standard items.

b. Power supply

The detector can operate on 115 ac line voltage, external 28-V dc, and on internal ± 12-V NiCd batteries. Due to its low power requirements of approximately 30 to 50 mW, the detector can be operated for approximately 200 hr on one battery charge. Operation is also possible during charge. A protection circuit cuts the batteries off when the voltage drops below 9 V. A battery voltage check is also provided. In a space capsule, the detector would be operated on the 28-V dc space capsule power supply. We therefore also provided for operation on external 28-V dc. This input is isolated by a dc-dc converter. For more details, see the detailed circuit diagram in Fig. 28.

c. Indicating circuit

The current through the potentiostatically controlled electrochemical cell is a direct measure for the electrochemical oxidation of carbon monoxide. This current is measured by a current-to-voltage converter which keeps the working electrode effectively at ground level. Adjustment of the output range and the temperature compensation are achieved by varying the feedback loop of the current-to-voltage converter. The output terminals were adjusted to deliver 0 to 100 μA and 0 to 5 V for CO concentrations of 0 to 60 ppm.

d. Temperature compensation

Since the CO detection current is temperature dependent, it is necessary to either control the temperature of the electrochemical cell or to compensate the output signal for the temperature effect. The latter approach was followed here.

A thermistor shows, except for the sign and slope, the same linear temperature relationship in an Arrhenius diagram as the detection current. Therefore, a thermistor is ideally suitable to be used as a variable component in the feedback loop of the current-to-voltage converter. The thermistor was located in the top of the electrochemical cell directly in the incoming gas stream. The slope adjustment without sacrifice in signal linearity was achieved by a variable series resistance.

B. Preliminary Test Results

Preliminary testing was directed primarily toward three critical areas of performance, namely, temperature dependence, response time, and long-term stability.

The sensing electrode (TFE 20/20 I) had been in constant operation for nearly 3 mo prior to mounting in the detector and had been used to study such parameters as dependence of signal on temperature, humidity, and potential (see Fig. 21). These somewhat rigorous experiments did not affect any permanent change in the performance characteristics of the electrode. The only corrective measure taken was to remove surface oxides (formed at the more anodic operating potentials) by cathodic stripping. This was sufficient to restore the electrode to its full capacity.

After mounting in the detector, the cell was placed on potentiostatic control and flushed with 50 ppm CO. The gain control was adjusted to the proper signal (4.2 V), and after 24 hr of continuous exposure, there was no decay of signal.

The detector was then placed in a 10°C thermostat and, after complete equilibration, was reexposed to 50 ppm CO. The signal remained constant at the original value throughout the 45-min exposure. This signified that proper temperature compensation over the range of 10° to 26°C had been achieved. The signal continued to remain constant during subsequent warmup and 18-hr exposure at ~25° (room temperature).

The typical response time of the instrument was found to be 1 min to 90% of full scale and 3 to 4 min to full scale. The same response time was observed upon removal of CO. In the absence of CO, the background signal was 0.1 V. The sensitivity was better than ± 1 ppm CO and the accuracy better than ± 2% of full scale. Operation of the detector on batteries or line voltage had no effect on the CO detection signal.

As a final test of long-term stability, the detector was continuously exposed to 50 ppm CO in air for a period of approximately 100 hr with no noticeable signal decay.

VI. REFERENCES

1. F. G. Will, J. Electrochem. Soc., 110, 145 (1963).
2. A. B. LaConti and H. J. R. Maget, J. Electrochem. Soc., 118, 506 (1971).
3. P. Stonehart, Electrochim. Acta, 12, 1185-1198 (1967).
4. J. Giner and C. Hunter, J. Electrochim. Soc., 116, 1124 (1969).